nanomaterials

MDPI

Review

Recent Advances in Monitoring Stem Cell Status and Differentiation Using Nano-Biosensing Technologies

Wijin Kim [1,†], Eungyeong Park [2,†], Hyuk Sang Yoo [1,3], Jongmin Park [2], Young Mee Jung [2,3,*] and Ju Hyun Park [1,*]

[1] Department of Biomedical Science, Kangwon National University, Chuncheon 24341, Gangwon-do, Korea
[2] Department of Chemistry, Kangwon National University, Chuncheon 24341, Gangwon-do, Korea
[3] Kangwon Radiation Convergence Research Support Center, Kangwon National University, Chuncheon 24341, Gangwon-do, Korea
* Correspondence: ymjung@kangwon.ac.kr (Y.M.J.); juhyunpark@kangwon.ac.kr (J.H.P.); Tel.: +82-33-250-8495 (Y.M.J.); +82-33-250-6566 (J.H.P.)
† These authors contributed equally to this work.

Abstract: In regenerative medicine, cell therapies using various stem cells have received attention as an alternative to overcome the limitations of existing therapeutic methods. Clinical applications of stem cells require the identification of characteristics at the single-cell level and continuous monitoring during expansion and differentiation. In this review, we recapitulate the application of various stem cells used in regenerative medicine and the latest technological advances in monitoring the differentiation process of stem cells. Single-cell RNA sequencing capable of profiling the expression of many genes at the single-cell level provides a new opportunity to analyze stem cell heterogeneity and to specify molecular markers related to the branching of differentiation lineages. However, this method is destructive and distorted. In addition, the differentiation process of a particular cell cannot be continuously tracked. Therefore, several spectroscopic methods have been developed to overcome these limitations. In particular, the application of Raman spectroscopy to measure the intrinsic vibration spectrum of molecules has been proposed as a powerful method that enables continuous monitoring of biochemical changes in the process of the differentiation of stem cells. This review provides a comprehensive overview of current analytical methods employed for stem cell engineering and future perspectives of nano-biosensing technologies as a platform for the in situ monitoring of stem cell status and differentiation.

Keywords: stem cell differentiation; single-cell level monitoring; single-cell RNA sequencing; optical spectroscopy; fluorescence; Raman; SERS

Citation: Kim, W.; Park, E.; Yoo, H.S.; Park, J.; Jung, Y.M.; Park, J.H. Recent Advances in Monitoring Stem Cell Status and Differentiation Using Nano-Biosensing Technologies. *Nanomaterials* **2022**, *12*, 2934. https://doi.org/10.3390/nano12172934

Academic Editor: Antonino Gulino

Received: 29 July 2022
Accepted: 23 August 2022
Published: 25 August 2022

1. Introduction

Stem cells can be distinguished from somatic cells by their unique abilities to self-perpetuate and differentiate into various cell types consisting of adult tissue or organ. Stem cell behaviors, including self-renewal and differentiation, are significantly affected by a multitude of physicochemical cues, such as cell–cell and cell–extracellular matrix interactions [1], topography, and stiffness of the matrix [2,3], and cellular signaling induced by soluble cues, such as cytokines and growth factors [4,5]. These complexities in lineage commitments can result in the heterogeneity of differentiation in certain stem cell populations. Despite technical advances in controlling the developmental processes of stem cells, the differentiation into unintended lineages and the existence of undifferentiated stem cells are regarded as major obstacles to the clinical application of stem cells in regenerative medicine. In stem cell transplantation therapies, unexpected cell types can emerge during differentiation. These might cause critical problems, such as tumorigenesis [6,7].

To meet clinical needs, the exhaustive monitoring of biodistribution, engraftment, viability, and differentiation into a target lineage of transplanted stem cells is required to

ensure bio-safety and to improve their therapeutic efficacy [8,9]. Up-to-date, different analysis methods of lineage-specific marker expression, such as immunostaining, Western blot, flow cytometry, and quantitative polymerase chain reaction (qPCR), have been widely used to characterize and monitor the differentiation process of stem cells [10,11]. Nevertheless, such conventional methods have some limitations due to their requirement of destructive steps, such as cell fixation and lysis, which can disrupt the spatial information in the differentiating cell population, thereby impeding longitudinal tracking from parental cells to their progenies [12–14]. A limitation to precise single-cell-level analysis during in vitro and in vivo differentiation due to the low resolution of the abovementioned methods is another important problem encountered in the in situ monitoring of stem cell differentiation. These limitations have compelled us to develop novel analytical methods that enable the highly sensitive in situ monitoring of stem cell differentiation at the single-cell level without any destructive steps.

The main purpose of this review is to recapitulate the latest advances in the development of technologies for tracking the lineage commitment of these stem cells, along with the necessity of monitoring their status and differentiation for clinical applications. In particular, we specifically discuss methods for the in situ monitoring of stem cell differentiation using nano-biosensing platforms, such as fluorescence-based nanotechnologies and Raman spectroscopy.

2. Clinical Application of Various Stem Cells and Necessity of Monitoring Differentiation Process

For clinical application, two types of stem cells have been widely studied: (1) mesenchymal stem cells, a type of adult stem cell that includes bone marrow-derived mesenchymal stem cells (BM-MSCs), dental pulp stem cells, (DPSCs), and adipose-derived stem cells (ADSCs); (2) pluripotent stem cells, such as embryonic stem cells (ESCs) and induced pluripotent stem cells (iPSCs). Here, we elaborate the use of these stem cells in regenerative medicine for disease treatments and the necessity of monitoring and controlling their differentiation processes for clinical applications (Figure 1).

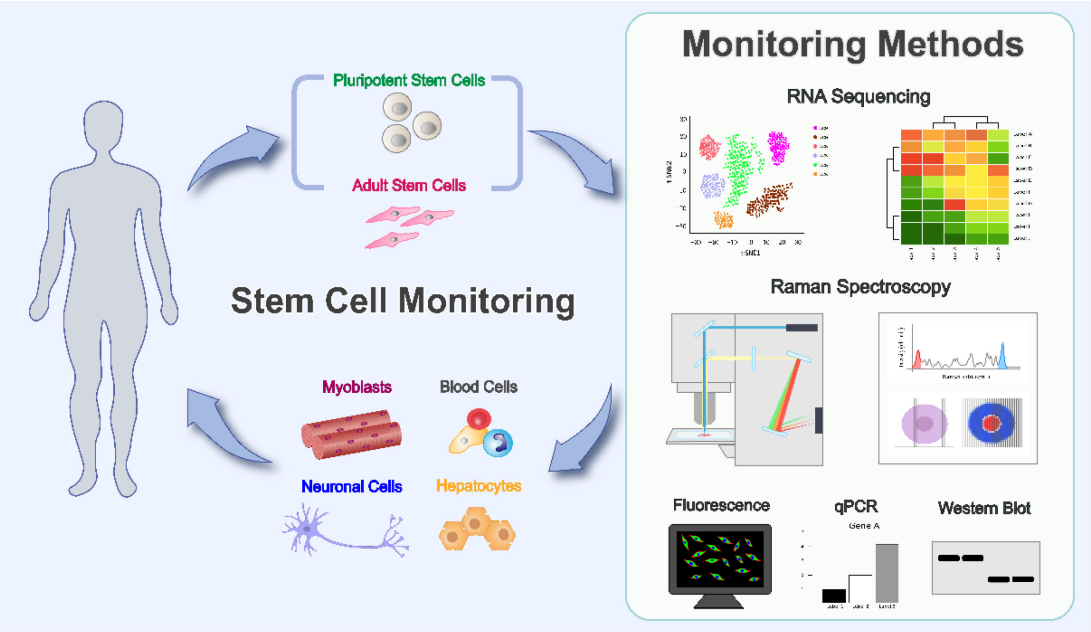

Figure 1. Schematic of the process of cell therapy using various stem cells and methods of tracing the lineage of these stem cells.

2.1. Mesenchymal Stem Cells

In a series of historic studies in the 1960s and 1970s, Friedenstein et al. identified MSCs as a fibroblast-like non-hematopoietic population that could differentiate into bone in the bone marrow [15,16]. Since then, MSCs have also been isolated from other tissues such as umbilical cord blood [17,18], peripheral blood [19,20] skin and muscle [21], dental pulp [22,23], lung [24], and adipose tissue [25]. Many comparative studies have suggested that MSCs isolated from different tissues share common properties such as the expression of MSC-specific genes and differentiation potential toward specific lineages despite slight differences in the population numbers, growth rate, and therapeutic outcomes [26–28]. In addition to their capabilities of self-renewal and differentiation into multi-cell types, MSCs possess the abilities of migrating toward injured tissues (called a homing effect [29]), activating resident cells, and modulating immune responses via paracrine action [30,31]. These versatile properties enable MSCs to be utilized as an appropriate resource for regenerative medicine.

As a result of a search using "mesenchymal stem cells" as the keyword in ClinicalTrials.gov, a total of 907 clinical trials, including completed cases, were found to be registered in different phases. The indications registered for MSC-transplantation therapy include neurological disorders, such as spinal cord injury [32], multiple sclerosis, and stroke [33,34], bone and cartilage diseases, such as osteoarthritis and rheumatoid arthritis [35,36], and cardiovascular diseases [37]. Because of their differentiation potential, the therapeutic effect of MSC transplantation was attributed to the differentiation of MSCs engrafted in the injured area into damaged cells and the subsequent tissue regeneration at the early stage of clinical trials [38]. However, other studies have revealed that in vivo engraftment and differentiation into the target lineage of transplanted MSCs is usually very inefficient for having a therapeutic impact, suggesting that the main effect of MSC transplantation might not be due to their differentiation [39,40]. Preferably, many reports have demonstrated that paracrine factors secreted from transplanted MSCs play a crucial role in tissue repair and regeneration [41,42].

In addition to the ambiguity of the mode-of-action of MSC transplantation therapies, safety issues regarding the quality control of MSCs have been debated. Other failure cases have also been reported in many clinical trials despite many successful outputs of preclinical studies and small-scale clinical trials at the laboratory level [43,44]. One of the most important factors attributed to the clinical failure of these therapies is the heterogeneity in the cell population and the differentiation capability of the MSCs. Many studies have demonstrated that MSCs obtained from different donors exhibit significant discrepancies in the proliferation rate and potential for differentiation into specific lineages, resulting in deviations in the clinical efficacy of MSC therapies [45,46]. The heterogeneity of MSCs is affected by not only donors but also by the tissue source, cell isolation, culture conditions, preservation, cell populations, and the passage number of in vitro cultures [47–49]. The functional heterogeneity of transplanted MSCs can provoke poor engraftment and uncontrolled differentiation, resulting in not only insignificant therapeutic efficacy but also severe side effects. The potential side effects of MSC transplantation include abnormal immune responses, malignant transformation, and prothrombotic disorder [50,51].

To overcome the potential risks of MSC therapies, it is crucial to monitor the cell characteristics and differentiation. In addition to the abovementioned conventional methods such as immunostaining, Western blotting, qPCR, and flow cytometry analysis, another generally accepted method is to examine the metabolites specific to each differentiated cell type derived from MSCs, such as calcified matrices of osteoblasts [52], lipid droplets of adipocytes [53], and sulfated proteoglycans of chondrocytes [54,55]. However, these methods are destructive, with serious limitations in the analysis of in vivo differentiation. For more precise identification of the heterogeneous cell population derived from MSCs, the development of non-destructive analytical techniques capable of monitoring multiple cell type-specific markers simultaneously at the single-cell level is strongly required.

2.2. Embryonic Stem Cells and Induced Pluripotent Stem Cells

Pluripotent stem cells (PSCs) can proliferate unlimitedly and differentiate into all kinds of lineages consisting of adult tissue. ESCs and iPSCs are included in the category of PSCs. Since the first human ESC line was established by James Thomson and colleagues [56], the clinical application of ESCs has been explored for several incurable diseases, such as age-related macular degeneration, Parkinson's Disease, and spinal cord injury [57]. To overcome the ethical dilemma of ESC-based therapy regarding the destruction of a human embryo and the requirement of numerous eggs in the establishment of an ESC line, a novel study delivered four specific factors to terminally differentiated somatic cells and reprogrammed them into a new type of PSCs called iPSCs [58]. Although a study suggested the clinical application of human iPSCs [59], they face many obstacles, such as the tumorigenicity and heterogeneity encountered by ESCs as well.

The risk of tumorigenicity due to the remaining undifferentiated cells is considered to be the most significant problem in the clinical application of PSC technology. Unlimited self-renewal is an important advantage in that enough cells for transplantation can be easily obtained. However, this property also results in a crucial problem because undifferentiated PSCs tend to proliferate infinitely even in vivo. Even if a few residual undifferentiated PSCs are administrated into a patient's body, they could induce the formation of teratoma, a type of germ tumor that contains all three germ lineages simultaneously [60]. Tumorigenesis might also arise from incorrectly patterned PSCs. For example, it has been reported that the epigenetic variation among human iPS cell lines is correlated with the differentiation capacity, indicating that a PSC line with certain epigenetic characteristics is inevitably incomplete in the differentiation into a specific lineage. The resulting differentiated cells may induce tumorigenesis when transplanted in vivo [61]. Aside from tumorigenicity, the functional heterogeneity among different PSC lines due to epigenetic variations might also impede quality control for uniform and predictable therapeutic efficacy.

For these reasons, precise screening is strongly required to satisfy the safety standards for the clinical application of PSC-based therapy. To select maturely differentiated cells or eliminate incorrectly differentiated PSCs, single-cell labeling techniques using monoclonal antibodies for cell surface markers have been studied. In clinical studies for treating ocular disorders, Nishida and colleagues found a novel surface marker for the elimination of both undifferentiated human iPSCs and non-corneal epithelial cells (CECs), including other cell types of iPSC-derived retinal lineage. As a result, the risk of tumorigenesis could be reduced in iPSC-derived CEC transplantation therapy [62,63]. However, these methods still could not completely eliminate undifferentiated and/or incorrectly differentiated PSCs. Therefore, as in the case of MSCs, the development of an advanced in situ monitoring system for PSC differentiation is necessary.

3. Latest Technological Advances in Monitoring Stem Cell Status and Differentiation

3.1. Tracing Differentiation of Stem Cells at the Single-Cell Level Using Single-Cell RNA Sequencing (scRNA-seq)

With advances in molecular biology, the states of differentiating cells can be identified by investigating the expression of marker genes using immunostaining or qPCR analysis. At present, scRNA-seq capable of massive gene expression profiling at the single-cell level provides novel opportunities to analyze stem cell heterogeneity [64,65]. scRNA-seq enables the simultaneous investigation of transcripts in numerous individual cells, which allows for the tracing of the differentiation trajectory in a heterogeneous cell population. In addition, scRNA-seq can provide precise information about 'off-target' cell types that emerge during differentiation. Although conventional immunostaining is useful for identifying target cells generated through differentiation using lineage-specific markers, it is difficult to distinguish non-differentiated cells and off-target cells, which are cell types differentiated into other undesired lineages [66]. Reconstructing differentiation through scRNA-seq can provide opportunities to ameliorate the differentiation protocol. Some recent studies have mapped differentiation trajectories and found crucial molecular markers related to the

bifurcation of lineages. By investigating a transcriptomic signature during mesendoderm to definitive endoderm (DE) development from the pluripotent state of human ESCs by scRNA-seq, Chu et al. identified a novel transcriptional regulator that governs the fate of ESCs into DE [67]. The single-cell mapping of the lineage bifurcation in the ectodermal differentiation of ESCs has revealed detailed profiles of distinct transcription factors in each lineage that emerged during early brain development, such as forebrain and mid/hindbrain lineages [68,69]. These results can provide strategies for the precise control of differentiation by stimulating target lineages while suppressing off-target lineages.

3.1.1. Cell Fate Mapping by Cellular Barcoding

Recently, cellular barcoding technology has emerged as an efficient tool for the precise lineage tracing of stem cells by scRNA-seq [70]. In this strategy, the genome of each individual cell is tagged with a specific DNA sequence of a given number of base pairs. According to the length of the DNA sequence, an almost infinite number of cells can be barcoded with a distinct heritable DNA tag. The barcoding of individual cells facilitates lineage reconstruction by identifying the progeny of a particular cell labeled with a specific tag. To introduce heritable genetic barcodes, some strategies have been utilized. The most widely used method so far relies on the manipulation of the vector pool encoding unique DNA sequences, such as viruses and plasmids [71,72]. Each vector can deliver the DNA tag into an individual cell through viral or non-viral transfection. The transfected cell is thereby labeled by the unique DNA barcode [73–76]. Recent advances in CRISPR-based genome editing technologies have facilitated efficient barcode generation. The initial strategy of CRISPR/Cas9-mediated cellular barcoding relied on a repair mechanism of Cas9-induced double-strand breaks in genomic DNA by nonhomologous end-joining with a subsequent introduction of short random insertions and deletions (INDELs) at the repair loci [77]. These random mutations by INDELs at a parental genome play the role of a barcode for distinguishing cells. To increase barcode diversity, Kalhor et al. proposed a strategy of evolving DNA barcodes that can alter their genetic code gradually [78]. In this system, a guide RNA (gRNA) is engineered to target its own locus introduced in the genome during the delivery of external genes encoding the gRNA. As a result, a mutation is created within the gRNA genomic locus. Subsequently, new gRNA expressed from the mutated locus leads to another mutation at its own gRNA locus. During each cell cycle, a series of these mutations generate highly diverse and evolving DNA barcodes that can be used to be deciphered by scRNA-seq.

3.1.2. Challenges of scRNA-seq-Based Differentiation Tracing

Despite its feasibility as a tool for tracing the stem cell differentiation trajectories and mapping cell fate, scRNA-seq has some limitations, including a considerable process time and cost [79,80]. One key limitation is that most scRNA-seq procedures require the disruption of tissue integrity and cell destruction, which can result in the loss of the spatial information in heterogenous cell populations [81,82]. During stem cell differentiation, each cell communicates with neighboring cells. Physicochemical interactions that trigger lineage commitment are significantly affected by an organized microenvironment. Spatial information that indicates which types of neighboring cells the cell to be tracked is in contact with (e.g., cells differentiated into the target lineage or off-target cells) is also crucial for the lineage commitment of stem cells, as is genomic or transcriptomic information. Thus, the loss of spatial information due to the destructive nature of scRNA-seq makes it difficult to trace cell fate and find crucial factors affecting differentiation into a specific lineage.

The requirement of genetic manipulation in DNA-barcoding before scRNA-seq-based lineage tracing and its low efficiency are other important technical obstacles. To transduce hard-to-transfect cells, such as human PSCs, with a barcode-expressing construct, a high multiplicity of infection and multiple rounds of infection with retrovirus or lentivirus are required, which can result in severe cell death [83]. In the case of CRISPR barcoding

methods, the potential off-target genetic mutations due to residual endonuclease activity might be an important reason for disturbing the developmental dynamics of stem cells.

In addition, the incomplete detection of unique barcode sequences, which can arise from a low signal-to-noise ratio of barcode readout or the endogenous knockout of transgenes, can distort the results of differentiation tracing [73]. Failure to capture and label even only a small fraction of the entire cell population might also skew the interpretations of scRNA-seq data [84]. Genetically unrelated cells are labeled with identical barcode sequences (barcode homoplasy), which can also cause the failure of cell fate monitoring in heterogeneous stem cell differentiation.

3.2. Fluorescence Spectroscopy to Monitor Stem Cell Differentiation

In the field of bioscience, the fluorescence imaging technique is widely used as a valuable tool to monitor the expression of target proteins, cellular processes, and cell dynamics [85,86]. It can also be used to visualize single cells, tissue, organs, or a whole body in real-time [87,88]. Fluorophore or fluorescent proteins are essential for applying this method to the detection of a target protein. In this method, when excitation photons are irradiated, emission photons are emitted from the fluorophore [89,90]. Fluorescence studies using immunohistochemistry and nanomaterials have been performed.

3.2.1. Immunocytochemistry (ICC)

ICC is the most used fluorescence protocol. It can evaluate the populations of stem cells. In this method, the secondary antibody with fluorescent tags detects the primary antibody bound to the target protein. For successful immunocytochemistry, it is important to select antibodies that can specifically bind to the target [91]. Based on previous studies, various proteins, such as TRA-1-60 [92], SSEA-4 [93,94], Sox2 [95], Oct4 [96,97], and Sushi-containing domain 2 [98], are markers for PSCs. Antibodies suitable for such proteins are usually used for fluorescence imaging [99]. Table 1 summarizes the studies that have monitored the differentiation process of stem cells over the past three years using immunocytochemistry [95,98,100–136]. ICC is a non-destructive method, different from Western blot.

Table 1. Recent studies related to stem cell differentiation using immunocytochemistry.

Stem Cell	Cell Source	Target Lineage
Adipose-derived stem cell (ADSC)	Human ADSC	Human Schlemm's canal cell [100]
Dental pulp stem cell (DPSC)	Human DPSC	Motor neuron cell [101]
	Human DPSC	Osteogenic cell [102,103]
	DPSC, dental follicle stem cells, periodontal ligament stem cell	Osteogenesis [104]
Embryonic stem cell (ESC)	Mouse ESC	Neural crest cell [105]
	Mouse ESC	Neuron [106]
	Mouse ESC	Embryoid body [107]
	Human ESC	Retinal pigment epithelial [108]
	Human ESC	Somatic cell [98]
Induced pluripotent stem cell (iPSC)	Human iPSC	Neural crest stem cell [95]
	Human peripheral blood mononuclear cell	iPSC [109]
	Human iPSC	Neuron [110,111]
	Human iPSC	Neuron [112]
	Human iPSC	β-cell [113]
	Human iPSC	Cardiomyocyte [114]

Table 1. *Cont.*

Stem Cell	Cell Source	Target Lineage
Mesenchymal stem cell (MSC)	Human adipose-derived (AD)-MSC	Cardiomyocyte [115]
	Human umbilical cord (UC)-MSC	Retinal pigment epithelial [116]
	Human UC-MSC	Chondroprogenitor [117]
	Human bone marrow (BM)-MSC	Neuron [118]
	Mouse MSC	Bone [119]
	Rat BM-MSC	Neurosphere [120]
	Rat BM-MSC	Bone [121]
	Human MSC	Nucleus pulposus-like cell [122]
	Mouse BM-MSC	β-cell into pancreatic lineage [123]
	Human AD-MSC	Pancreatic cell [124]
	Human MSC	Osteogenic and chondrogenic lineage [125]
	Human MSC	Cardiac cell [126]
	Rat BM-MSC	Adipogenic and chondrogenic cell [127]
Neural stem cell (NSC)	Rat NSC	oligodendrocyte [128]
	NSC	Neuron [112,129–131]
	Premigratory neural crest stem cell	Enteric neuron [99]
	Monkey NSC	Neuronal cell, glial cell [132]
	Rat NSC	Neuron [133]
	Human NSC	Neuron [134]
	NSC/progenitor cell	Neuron [135]
Parthenogenetic stem cell	Mouse parthenogenetic stem cell	Cardiomyocyte [136]

3.2.2. Nanomaterials in Fluorescence-Based Biosensing

Nanomaterials have optical properties, such as photostability and the control of excitation and emission wavelengths [137]. Fluorescent nanoparticles can be monitored for a long time due to their long stability in cells. Graphene quantum dots (GQDs), a type of nanomaterial, have been used as fluorescent materials because they can maintain excellent photoluminescent and photostability [138,139]. To improve their biocompatibility, GQDs have been combined with biochemically inert polyethylene glycol (PEG) [140]. Ji et al. [140] reported that 320 μg/mL of PEG-GQDs did not affect the differentiation from rat neural stem cells to neurons or glial cells and that PEG-GQDs composites showed adequate bioimaging capabilities when they were internalized into neural stem/progenitor cells. The synthesis of fluorescent polymers with high stability and a high quantum yield has also been reported [141–143]. Jang et al. [143] reported that aggregation-induced emission nanoparticles (AIE-NPs) can penetrate greatly into cells. AIE-NPs in cells can be retained for a long time without altering the neuronal proliferation, differentiation, or viability in vitro. AIE-NPs labeled neuronal grafts were tracked for one month in mouse brain striatum at various time points after transplantation. Choi et al. [144] found that living human MSCs (hMSCs) could be differentiated into osteogenic lineage using polydopamine-coated gold (Au) nanoparticles (Au@PDA). To recognize a target mRNA, a hairpin DNA (hpDNA) strand with a fluorescent tag was immobilized at the PDA shell. Fluorescent signals were quenched by Au@PDA and recovered when the hpDNA was dissociated from the Au@PDA by the target miRNA. Au@PDA–hpDNA displayed fluorescence in hMSCs differentiated into primary osteoblasts. Using this phenomenon, the differentiation process could be monitored. In addition, some recent studies using DNA nanotechnology in combination with fluorescence spectroscopy as a tool for biosensing have been reported [145–147].

Although fluorescence signaling using monofunctional nanoparticles could be efficient for stem cell monitoring, some limitations still remain. Accordingly, studies on the fabrication and application of multifunctional nanoparticles have been widely conducted. Nanomaterial-based fluorescence dyes can be used in drug delivery and transplant treatment through monitoring while tracking in vivo mechanisms [148–151]. Li et al. [151] reported on a novel near-infrared (NIR) light-activated nanoplatform for the remote control of cell differentiation and the real-time monitoring of differentiation simultaneously. This was attained by encapsulating a photoactivatable caged compound (DMNPE/siRNA) and combining a matrix metalloproteinase 13 (MMP13) cleaved imaging peptide-tetraphenylethylene (TPE) unit conjugated with mesoporous silica-coated upconversion nanoparticles (UCNPs). When irradiated with NIR light, the photoactivated caged compound was activated and the siRNA was released from the UCNPs, enabling the controlled differentiation of stem cells by light. The MMP13 triggered by osteogenic differentiation effectively cleaved the TPE probe peptide, enabling the real-time monitoring of stem cell differentiation by aggregation-induced emission.

Gold nanoparticles (AuNPs) have been widely studied in medical fields, such as imaging, drug delivery, and theragnostic systems [152]. Wu et al. [153] developed multifunctional AuNPs to control cell fate and simultaneously detect the osteogenic differentiation of hMSCs in real time. AuNP-polyethyleneimine-peptide-fluorescein isothiocyanate/small molecule-interfering RNA (AuNP-PEI-peptide-FITC/siRNA) nanocomplexes to control the osteogenic differentiation of hMSCs could be silenced by the peroxisome proliferator-activated receptor γ (PPARγ), an adipogenesis-related gene. By measuring the activity of the MMP13 enzyme produced during osteogenic differentiation through the recovery of FITC fluorescence, it was demonstrated that AuNP nanocomplexes could control cell differentiation. They could be used as a nanoprobe for the real-time detection of the osteogenic differentiation of hMSCs.

3.3. Profiling and Tracing of Stem Cell Differentiation Using Raman Spectroscopy

Raman spectroscopy is a powerful method that can characterize cell information at the molecular level while obtaining images of stem cells at the same time [154–156]. It is based on inelastically scattered photons with different frequencies from excitation photons. It is the change in the wavelength of the scattered photon that provides the chemical and structural information [157]. Therefore, Raman spectroscopy reflects the fingerprint region of the target [158–161]. Raman spectroscopy is suitable for the long-term monitoring of cellular processes due to its advantages such as light stability [161] and no need for antibodies [162].

3.3.1. Raman Spectroscopy for Identification of Stem Cell Differentiation

Monitoring the stem cell differentiation process by Raman spectroscopy has been very actively studied in the last decade. Generally, the Raman spectrum of a cell is described as a typical fingerprint including the nucleic acid (at 720–820 and 1080–1100 cm^{-1}), lipid (1310 and 1440 cm^{-1}), protein (1030, 1170–1210, and 1610–1660 cm^{-1}), and amino acid residue (e.g., phenylalanine, 1002 cm^{-1}) (Figure 2) [163–165]. However, the position and intensity of the Raman bands are different for each cell because the cell components are different. The analysis of a Raman spectrum of a stem cell that contains various chemical compounds is very complicated. Therefore, multivariate analyses, such as principal component analysis (PCA), have been applied to identify and distinguish the differentiation of stem cell processes [166–168].

Lazarevic et al. [166] investigated stem cell differentiation to adipogenic, chondrogenic, and osteogenic lineage using micro-Raman spectroscopy. The relative intensities of bands corresponding to nucleic acids and proteins can distinguish the state of adipogenic differentiation. During adipogenic differentiation, the intensities of the nucleic acid bands decrease, while those of the protein and lipid bands increase. The amounts of protein and proteoglycan increased during the chondrogenic differentiation. In the case of osteogenic

differentiation, the spectral difference between human periodontal ligament stem cells (hPDLSCs) and osteoblasts was due to decreases in the band intensities of amino acids and lipids and increases in the band intensities of carbonates and phosphates.

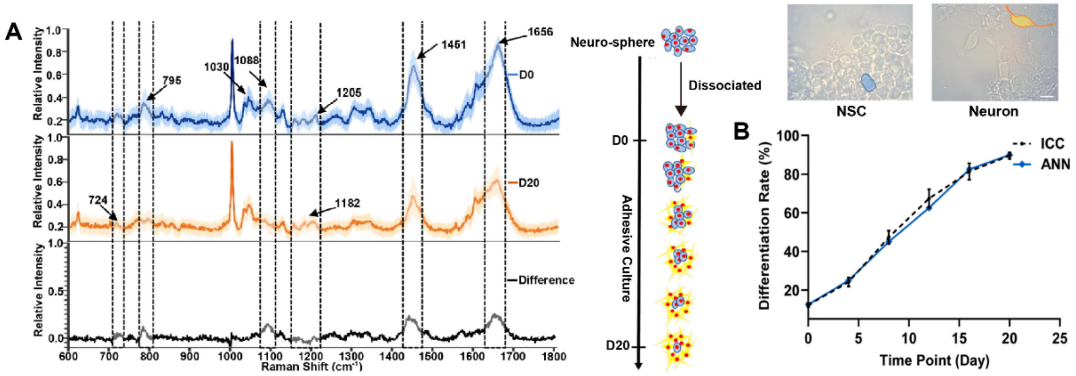

Figure 2. (**A**) Raman spectra of stem cells on day 0 (blue) and day 20 (yellow). The black spectrum shows differences. (**B**) Evaluation of differentiation rate using machine learning based on Raman spectra. Adapted with permission from Ref. [163]. Copyright 2021 American Chemical Society.

During the differentiation of stem cells into neurons, the intensity of the lipid band decreases, while that of the protein increases. Based on these results, it was found that 12% of stem cells on day 0 already started toward neuron differentiation, whereas 10% of the cells did not differentiate after 20 days. To improve the prediction of the differentiation rate, an artificial neural network (ANN) was used. An ANN is a machine learning method that can provide a non-invasive classification of cell types at the single-cell level [163]. Compared to the Raman spectrum of a neuron cell, a band at 480 cm^{-1} assigned to glycogen appeared in the Raman spectrum of the iPSC [167].

Undifferentiated myoblast cells and myoblast cells differentiated at three different stages can be easily distinguished using deep UV resonance Raman spectroscopy combined with chemometric techniques [168]. Mandair et al. [169] reported that bone tissue formed in an osteogenic cell culture exhibited progressive matrix maturation and mineralization. However, they could not fully replicate the high degree of collagen fibril order found in native bones.

Alraies et al. [170] reported on the discrimination between different DPSCs populations by DNA and protein using the averaged Raman spectrum of DPSCs. Simonović et al. [171] investigated the differentiation of three dental stem cells (apical papilla (SCAP), dental follicle (DFSC), and pulp (DPSC)) using the relative intensity ratio of the tryptophan band versus nucleic acid observed in their Raman spectra.

3.3.2. Raman Spectroscopy for Imaging Stem Cell Differentiation

Raman spectroscopy can be used to add image contrast to visualizing structures and dynamics in living systems and materials. Chemical composition is most commonly used to provide contrast for determining the spatial distributions of chemical components [172].

Ravera et al. [173] reported that Raman micro-spectroscopy can contribute to the understanding of biochemical evolution underpinning the cellular progression from an undifferentiated state to a condensation stage and then to a terminally differentiated state. To monitor the process of MSC differentiation into chondrocytes in vitro, Raman micro-spectroscopy was used, providing a holistic molecular picture of cellular events governing the differentiation. They found that the characteristic signatures of several specific macromolecules of the extracellular matrix (ECM) were identifiable in the early stages of condensation, including collagen type II, proteoglycans, adhesion molecules, and several other proteins, whereas, in the latter stages, the elaboration of the lipidic content of the ECM appeared to be the most significant. Using Raman imaging, De Bleye et al. [174]

monitored the synthesis of ECM and its progressive mineralization during the osteogenic differentiation process.

Raman spectroscopy can detect the osteogenic differentiation process of stem cells more sensitively than other chemical-based staining assays. Suhito et al. [52] reported on a new method capable of the in situ label-free quantification of stem cell differentiation into multiple lineages, even at a single-cell level. Based on Raman images, they found that the osteogenesis of hADSCs could be determined and quantified after 9 days of differentiation. This result is a week earlier than the typical Alizarin Red S (ARS) staining method. They [175] also reported a novel autofluorescence-Raman mapping integration analysis for the ultra-fast label-free monitoring of adipogenic differentiation (Figure 3). In this method, autofluorescence (AF) imaging based on endogenous fluorophores in cells enables the rapid visualization of the cell morphology and cytosolic microstructure, while Raman mapping based on a specific molecular signature can precisely identify the biological molecules of interest. This method can avoid the erroneous characterization of individual cells in the same batch or different batches.

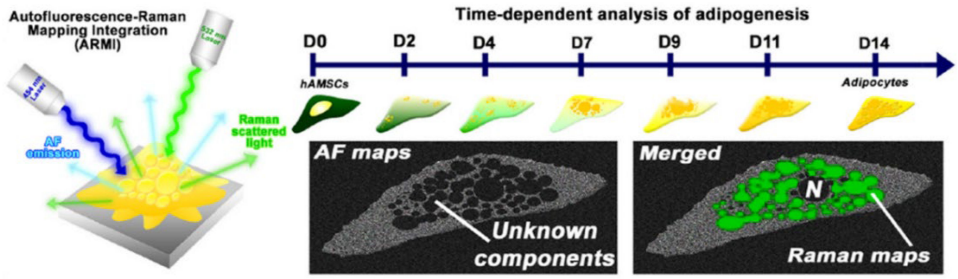

Figure 3. Schematic illustration of AF-Raman mapping analysis. Reprinted with permission from Ref. [175]. Copyright 2021 Elsevier.

Kim et al. [176] reported a 3D Raman mapping-based analytical method to identify crucial factors responsible for inducing variability in differentiated stem cell spheroids. They analyzed and monitored human DPSC spheroids based on three different Raman bands of hydroxyapatite (odontogenic differentiation marker), β-carotene (precursor of hydroxyapatite), and proteins/cellular components (cell reference) (Figure 4). Dou et al. [177] reported the diagnosis of the early-stage differentiation of mouse ESCs using Raman imaging. Raman imaging was used to characterize the spectral features of undifferentiated inner cells and peripheral cells of differentiated embryoid bodies. PCA was employed to obtain more differences and discriminate between the two cell types. Kukolj et al. [178] investigated inter-individual differences between BM-MSCs at a single-cell level by Raman spectroscopy. Despite having a similar biochemical background, fine differences in the Raman spectra of the BM-MSCs of each donor could be detected.

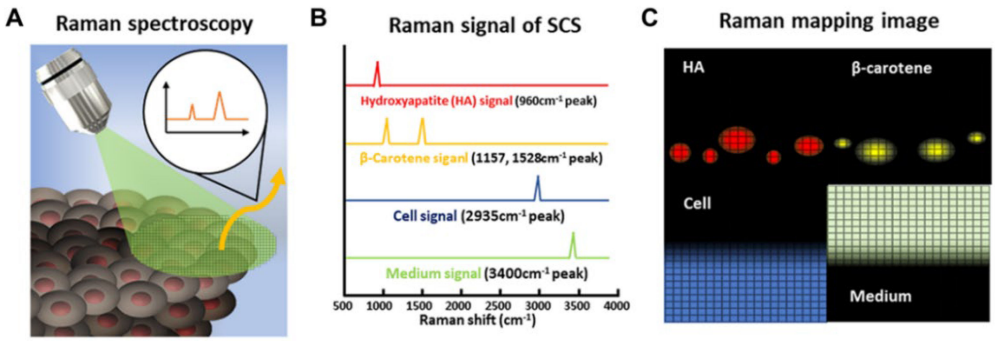

Figure 4. (**A**) Schematic illustration of 3D Raman mapping-based analytical method. (**B**) Characteristic peak of HA, β-carotene, cell, and medium. (**C**) 3D Raman mapping using specific peaks. Adapted with permission from Ref. [176]. Copyright 2021 American Chemical Society.

3.3.3. Surface-Enhanced Raman Spectroscopy (SERS)

Although Raman spectroscopy can be used for the identification and imaging of stem cells, it also has some limitations due to its low cross-section [179]. The low cross-section attenuates the signal-to-noise ratio, leading to an increase in measurement time. An extended measurement time not only causes serious damage to the cells but also makes it difficult to measure a large number of cells [180]. Another limitation of Raman scattering is the difficulty of measuring subtle changes in the proteins and minerals. SERS is a promising technique that can compensate for this shortcoming. SERS is a phenomenon that can significantly enhance the Raman signal when molecules are absorbed or approached near the surface of metal nanoparticles [181]. It can detect even single molecules and is suitable for long-term monitoring [182]. Although roughed gold, silver, and copper metal surfaces have been used as typical SERS active substrates [183], recently, a SERS substrate was expanded with semiconductors, graphene, and quantum dot, which also show strong SERS enhancement [184]. For various purposes, SERS substrates can be fabricated in different sizes, shapes, and coatings [185].

There are two SERS strategies—labeled and label-free methods for detection with and without biomarkers, respectively. The label-free SERS method provides rich stem cell information for identification without labeling the analytes [186–192]. In this method, the information of the biomacromolecules, such as the protein structure, nutrient amounts, and biological processes occurring at the cellular level that change during differentiation, can be detected. Milewska et al. [189,192] reported on the differentiation of BM-MSCs using label-free SERS. They examined the bands of cholesterol, proteins, collagen backbone, proline, calcium hydroxyapatite, and a phospholipid alkyl chain for SERS mapping (Figure 5) [192]. BM-MSCs cultured on a biocompatible nanostructured gold substrate for 7 and 21 days revealed different stages of the differentiation spectrum of individual cells, such as molecular species and chemical events on the cellular membrane [189,192].

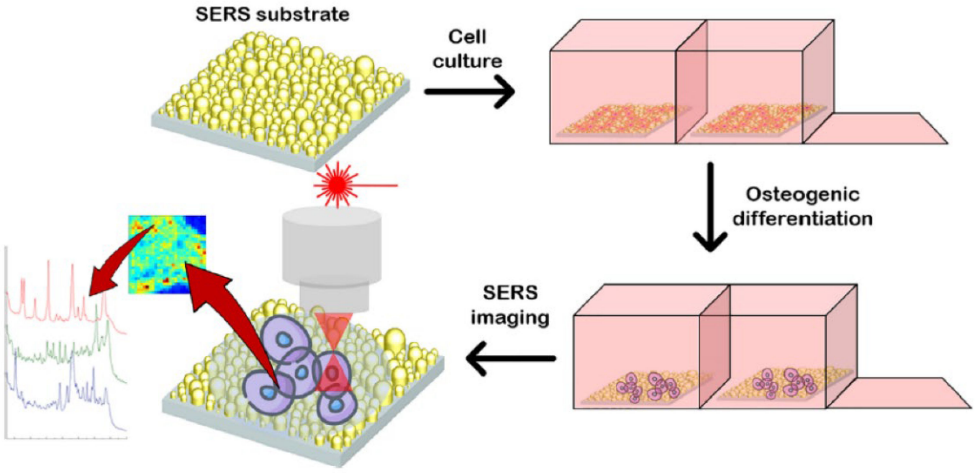

Figure 5. Schematic illustration of label-free SERS monitoring differentiation of BM-MSCs using gold substrate. Adapted with permission from Ref. [192]. Copyright 2021 American Chemical Society.

SERS can also be applied to biological processes occurring inside stem cells [191]. The profiling of molecular changes in the nucleus of a single DPSC was monitored by AuNPs functionalized with a cell-penetrating peptide. Wang et al. [191] identified the differentiation process of DPSCs stimulated by drugs. Using label-free SERS, they found that two pivotal differentiation biomarkers, alkaline phosphatase (ALP) and dentin sialophosphoprotein (DSPP), were overexpressed during the process. The corresponding transformation of the DNA/RNA backbone vibrational modes was also observed during the differentiation process, indicating the occurrence of the replication or transcription of the DNA.

Indirect SERS methods have also been widely studied because label-free SERS spectra are too complex for analyzing specific targets [179,193]. Choi et al. [194] developed a graphene oxide (GO)-hybrid nano-SERS array to detect dopamine (DA) that can characterize the differentiation of neural stem cells (Figure 6). During neural differentiation, the DA was complexed with a DA-binding DNA aptamer conjugated with Raman dye and released from the hybrid nano-SERS array. As a result, the degree of differentiation of the neural stem cells was evaluated from the decreased SERS signal. This developed SERS-based detection method can investigate single-cell signaling pathways associated with DA or other neurotransmitters and their roles in neurological processes.

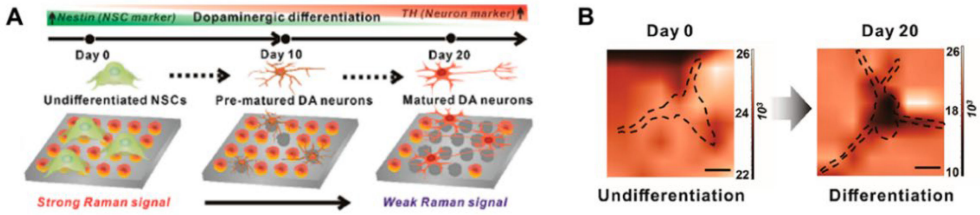

Figure 6. (**A**) Schematic illustration of characterization of neural differentiation using GO-hybrid nano-SERS array. (**B**) SERS mapping imaging before and after neural differentiation. Adapted with permission from Ref. [194]. Copyright 2020 American Chemical Society.

Gold nanostructures (AuNPs), such as nanocages and nanostars, can be easily adjusted to expand the localized surface plasmon resonance (LSPR) to near-infrared (NIR). Nanocages facilitate efficient drug delivery to stem cells through a biocompatible interior hollow space [195]. Cao et al. [196] reported an ultrasensitive SERS method for the long-term detection and imaging of miR-144-3p in the osteogenic differentiation of BM-MSCs. They detected miR-144-3p, an osteogenic differentiation biomarker of BM-MSCs, using Au nanocage-hairpin DNA. They found that these nanoprobes were capable of the long-term tracking of the dynamic expression of miR-144-3p (21 days) in differentiating BM-MSCs.

In addition, nanostars not only have many sharp tips that can produce highly sensitive signals by forming strong LSPR, but also have a large surface area, allowing various biomolecules to connect to the surface [197,198]. Hua et al. [197] fabricated a gold nanostar (Au-Star)-based second near-infrared window (NIR-II) fluorescence/SERS dual-modal imaging probe for the labeling and precise tracking of stem cells. Using this imaging approach, stem cells in hypodermic and myocardial infarction models can be tracked with high resolution and depth-independent imaging capabilities.

3.4. Other Methods for Monitoring of Stem Cell Differentiation

Although optical spectroscopy is an attractive tool for monitoring stem cell differentiation, it may cause photodamage of cells [180]. To avoid the photodamage of cells, it is necessary to extend the range of the light source or optimize the procedure to reduce the measurement time. Here, we introduce other spectroscopic methods for monitoring stem cell differentiation.

3.4.1. Infrared (IR) Spectroscopy

IR spectroscopy is a powerful tool to characterize each cell type and state based on specific molecular properties represented by sensitive IR spectroscopic fingerprints. [199]. Since the energy of the excitation light source of IR spectroscopy is lower than that of Raman or fluorescence spectroscopy, it has a lower risk of photodamage [200]. IR spectroscopy can distinguish between stem cells and their derivatives.

Wang et al. [201] developed a single-cell Fourier transform infrared (FTIR) microspectroscopy based on the method for the quantitative evaluation of cellular heterogeneity by calculating the cell-to-cell similarity distance of IR spectral data. They obtained spectral mapping images of the hMSC differentiation based on 2940–2910 cm^{-1} (fatty acid), 1670–1600 cm^{-1} (protein), and 1133–1033 cm^{-1} (nucleic acid) and revealed that IR pheno-

types might reflect dynamic heterogeneity changes in the cell population during adipogenic differentiation. This is enough to measure the MSC, which has an average diameter of 18 µm. Gieroba et al. [202] used macro attenuated total reflection (ATR)-FTIR spectroscopic imaging for the analysis of a ceramic-based biomaterial (chitosan/β-1,3-glucan/hydroxyapatite). According to their study, this spectroscopic approach is very suitable for studying the formation of new bone tissue and ECM components because sample staining and demineralization are not required. Thus, this approach is rapid and cost-effective.

3.4.2. Second Harmonic Generation (SHG) Scanning

SHG is a nonlinear optical process that is sensitive to the symmetry of media [203]. SHG microscopy has been applied to various specimens, including biological samples such as collagen, myosin, and microtubules. SHG has the advantages of no bleaching, no blinking, no signal saturation, and a high signal-to-noise ratio compared to fluorescence. Qi et al. [204] demonstrated the possibility of the stem cell internalization of boron-doped graphene quantum dots (B-GQDs) as an SHG probe and showed no hindering of the central physiological activities of the stem cells, such as differentiation.

Ibrahim et al. [205] performed structural analysis using extracellular collagen alignment and the mineral density in bone tissue engineered samples to evaluate the osteogenic maturation of human hASCs. They demonstrated that altering the physical environment and introducing a blood supply can enhance the maturity of the bone to which these cells form. Kourgiantaki et al. [206] demonstrated that grafts based on porous collagen-based scaffolds, similar to biomaterials utilized clinically in induced regeneration, can deliver and protect embryonic neural stem cells (eNSCs) at spinal cord injury (SCI) sites, leading to the significant improvement of locomotion recovery in an experimental mouse SCI model.

3.4.3. Hyperspectral Spectroscopy

Hyperspectral imaging (HSI) integrates conventional imaging and spectroscopy and is a label-free detection method [207]. Ogi et al. [208] reported on a label-free observation method for stem cell research that can classify neurons and glia in neural stem cell cultures using HSI microscopy combined with machine learning. Metha et al. [209] reported on a novel methodology using HSI combined with spectral angle mapping-based machine learning analysis to distinguish differentiating human ADSCs from control stem cells.

4. Conclusions

Uncontrolled differentiation is one of the major obstacles in stem cell transplantation therapies. For preventing phenotypical alterations, such as tumorigenesis and physiological heterogeneity, methods capable of accurate in vivo characterization of transplanted stem cells at the single-cell level are required. Recently, various strategies based on single-cell transcriptomics, such as scRNA-seq, have been developed to monitor the status of stem cells and predict their differentiation trajectories. Despite its excellence in facilitating cell fate mapping by providing enormous information about the transcriptome of a large population at the single-cell level, scRNA-seq has a crucial limitation in that it contains a cell disruption step, hindering the spatial information of particular cells as well as the in situ tracking of differentiation. As non-destructive alternatives, optical spectroscopies such as fluorescence, Raman, IR, SHG, and HSI, have been studied for monitoring with high sensitivity and accuracy at the single-cell level. Raman is a label-free method that can screen differentiation and obtain chemical information at the molecular level of stem cells, which can be used to discriminate stem cells according to their differentiation state. SERS has an enhanced Raman signal, thereby facilitating the detection of biomolecules, such as neurotransmitters, with more sensitivity. By examining Raman and SERS spectra with PCA and machine learning, many attempts have been made to determine the degree of stem cell differentiation and cluster each differentiation state. Although other limitations of spectroscopy-based techniques, such as long measurement times and low sensitivity in some cases, still remain, recent studies have attempted to overcome these limitations

by combining two or three spectroscopy methods simultaneously or utilizing artificial intelligence technology. In the future, technologies discussed in this review can be used as an advanced monitoring system for in vivo and in vitro studies for clinical applications using stem cells.

Author Contributions: Conceptualization, W.K., E.P., Y.M.J. and J.H.P.; resource, H.S.Y. and J.P.; writing—original draft preparation, W.K. and E.P.; writing—review and editing, Y.M.J. and J.H.P.; visualization, W.K., E.P., H.S.Y. and J.P.; supervision, Y.M.J. and J.H.P.; funding acquisition, Y.M.J. and J.H.P. All authors have read and agreed to the published version of the manuscript.

Funding: This research was supported by the Basic Science Research Program of the National Research Foundation (NRF) funded by the Korean Government (Ministry of Science and ICT) (Nos. 2020R1A4A1016093 and 2021R1A2C1010865).

Institutional Review Board Statement: Not applicable.

Informed Consent Statement: Not applicable.

Data Availability Statement: The original contributions presented in the study are included in the article.

Conflicts of Interest: All authors declare no conflict of interest.

References

1. Burdick, J.A.; Vunjak-Novakovic, G. Engineered microenvironments for controlled stem cell differentiation. *Tissue Eng. Part A* **2009**, *15*, 205–219. [CrossRef] [PubMed]
2. Engler, A.J.; Sen, S.; Sweeney, H.L.; Discher, D.E. Matrix elasticity directs stem cell lineage specification. *Cell* **2006**, *126*, 677–689. [CrossRef] [PubMed]
3. Mao, A.S.; Shin, J.-W.; Mooney, D.J. Effects of substrate stiffness and cell-cell contact on mesenchymal stem cell differentiation. *Biomaterials* **2016**, *98*, 184–191. [CrossRef] [PubMed]
4. Almalki, S.G.; Agrawal, D.K. Key transcription factors in the differentiation of mesenchymal stem cells. *Differentiation* **2016**, *92*, 41–51. [CrossRef] [PubMed]
5. Kristensen, D.M.; Kalisz, M.; Nielsen, J.H. Cytokine signalling in embryonic stem cells. *APMIS* **2005**, *113*, 756–772. [CrossRef]
6. Sato, Y.; Bando, H.; Di Piazza, M.; Gowing, G.; Herberts, C.; Jackman, S.; Leoni, G.; Libertini, S.; MacLachlan, T.; McBlane, J.W.; et al. Tumorigenicity assessment of cell therapy products: The need for global consensus and points to consider. *Cytotherapy* **2019**, *21*, 1095–1111. [CrossRef]
7. Barkholt, L.; Flory, E.; Jekerle, V.; Lucas-Samuel, S.; Ahnert, P.; Bisset, L.; Büscher, D.; Fibbe, W.; Foussat, A.; Kwa, M. Risk of tumorigenicity in mesenchymal stromal cell–based therapies—Bridging scientific observations and regulatory viewpoints. *Cytotherapy* **2013**, *15*, 753–759. [CrossRef]
8. Kircher, M.F.; Gambhir, S.S.; Grimm, J. Noninvasive cell-tracking methods. *Nat. Rev. Clin. Oncol.* **2011**, *8*, 677–688. [CrossRef]
9. Nguyen, P.K.; Riegler, J.; Wu, J.C. Stem cell imaging: From bench to bedside. *Cell Stem Cell* **2014**, *14*, 431–444. [CrossRef]
10. Martí, M.; Mulero, L.; Pardo, C.; Morera, C.; Carrió, M.; Laricchia-Robbio, L.; Esteban, C.R.; Belmonte, J.C.I. Characterization of pluripotent stem cells. *Nat. Protoc.* **2013**, *8*, 223–253. [CrossRef]
11. Nardi, N.B.; Meirelles, L. Mesenchymal stem cells: Isolation, in vitro expansion and characterization. *Stem Cells* **2008**, 249–282.
12. Ragni, E.; Viganò, M.; Rebulla, P.; Giordano, R.; Lazzari, L. What is beyond aq RT-PCR study on mesenchymal stem cell differentiation properties: How to choose the most reliable housekeeping genes. *J. Cell. Mol. Med.* **2013**, *17*, 168–180. [CrossRef]
13. Suhito, I.R.; Angeline, N.; Choo, S.-S.; Woo, H.Y.; Paik, T.; Lee, T.; Kim, T.-H. Nanobiosensing platforms for real-time and non-invasive monitoring of stem cell pluripotency and differentiation. *Sensors* **2018**, *18*, 2755. [CrossRef]
14. Kim, T.-H.; Yea, C.-H.; Chueng, S.-T.D.; Yin, P.T.-T.; Conley, B.; Dardir, K.; Pak, Y.; Jung, G.Y.; Choi, J.-W.; Lee, K.-B. Large-scale nanoelectrode arrays to monitor the dopaminergic differentiation of human neural stem cells. *Adv. Mat.* **2015**, *27*, 6356–6362. [CrossRef]
15. Friedenstein, A.; Chailakhjan, R.; Lalykina, K. The development of fibroblast colonies in monolayer cultures of guinea-pig bone marrow and spleen cells. *Cell Prolif.* **1970**, *3*, 393–403. [CrossRef]
16. Friedenstein, A.J.; Gorskaja, J.; Kulagina, N. Fibroblast precursors in normal and irradiated mouse hematopoietic organs. *Exp. Hematol.* **1976**, *4*, 267–274.
17. Lee, O.K.; Kuo, T.K.; Chen, W.-M.; Lee, K.-D.; Hsieh, S.-L.; Chen, T.-H. Isolation of multipotent mesenchymal stem cells from umbilical cord blood. *Blood* **2004**, *103*, 1669–1675. [CrossRef]
18. Bieback, K.; Kern, S.; Klüter, H.; Eichler, H. Critical parameters for the isolation of mesenchymal stem cells from umbilical cord blood. *Stem Cells* **2004**, *22*, 625–634. [CrossRef]
19. Zvaifler, N.J.; Marinova-Mutafchieva, L.; Adams, G.; Edwards, C.J.; Moss, J.; Burger, J.A.; Maini, R.N. Mesenchymal precursor cells in the blood of normal individuals. *Arthritis Res. Ther.* **2000**, *2*, 477. [CrossRef]

20. Villaron, E.M.; Almeida, J.; López-Holgado, N.; Alcoceba, M.; Sánchez-Abarca, L.I.; Sanchez-Guijo, F.M.; Alberca, M.; Pérez-Simon, J.A.; San Miguel, J.F.; Del Cañizo, M.C. Mesenchymal stem cells are present in peripheral blood and can engraft after allogeneic hematopoietic stem cell transplantation. *Haematologica* **2004**, *89*, 1421–1427.
21. Young, H.E.; Steele, T.A.; Bray, R.A.; Hudson, J.; Floyd, J.A.; Hawkins, K.; Thomas, K.; Austin, T.; Edwards, C.; Cuzzourt, J. Human reserve pluripotent mesenchymal stem cells are present in the connective tissues of skeletal muscle and dermis derived from fetal, adult, and geriatric donors. *Anat. Rec.* **2001**, *264*, 51–62. [CrossRef] [PubMed]
22. Gronthos, S.; Mankani, M.; Brahim, J.; Robey, P.G.; Shi, S. Postnatal human dental pulp stem cells (DPSCs) in vitro and in vivo. *Proc. Natl. Acad. Sci. USA* **2000**, *97*, 13625–13630. [CrossRef] [PubMed]
23. Gronthos, S.; Brahim, J.; Li, W.; Fisher, L.; Cherman, N.; Boyde, A.; DenBesten, P.; Robey, P.G.; Shi, S. Stem cell properties of human dental pulp stem cells. *J. Dent. Res.* **2002**, *81*, 531–535. [CrossRef] [PubMed]
24. Martin, J.; Helm, K.; Ruegg, P.; Varella-Garcia, M.; Burnham, E.; Majka, S. Adult lung side population cells have mesenchymal stem cell potential. *Cytotherapy* **2008**, *10*, 140–151. [CrossRef] [PubMed]
25. Zuk, P.A.; Zhu, M.; Ashjian, P.; De Ugarte, D.A.; Huang, J.I.; Mizuno, H.; Alfonso, Z.C.; Fraser, J.K.; Benhaim, P.; Hedrick, M.H. Human adipose tissue is a source of multipotent stem cells. *Mol. Biol. Cell* **2002**, *13*, 4279–4295. [CrossRef]
26. Kern, S.; Eichler, H.; Stoeve, J.; Klüter, H.; Bieback, K. Comparative analysis of mesenchymal stem cells from bone marrow, umbilical cord blood, or adipose tissue. *Stem Cells* **2006**, *24*, 1294–1301. [CrossRef]
27. Wagner, W.; Wein, F.; Seckinger, A.; Frankhauser, M.; Wirkner, U.; Krause, U.; Blake, J.; Schwager, C.; Eckstein, V.; Ansorge, W. Comparative characteristics of mesenchymal stem cells from human bone marrow, adipose tissue, and umbilical cord blood. *Exp. Hematol.* **2005**, *33*, 1402–1416. [CrossRef]
28. Uccelli, A.; Moretta, L.; Pistoia, V. Mesenchymal stem cells in health and disease. *Nat. Rev. Immunol.* **2008**, *8*, 726–736. [CrossRef]
29. Karp, J.M.; Teo, G.S.L. Mesenchymal stem cell homing: The devil is in the details. *Cell Stem Cell* **2009**, *4*, 206–216. [CrossRef]
30. Lin, F.; Moran, A.; Igarashi, P. Intrarenal cells, not bone marrow–derived cells, are the major source for regeneration in postischemic kidney. *J. Clin. Investig.* **2005**, *115*, 1756–1764. [CrossRef]
31. Liang, X.; Ding, Y.; Zhang, Y.; Tse, H.-F.; Lian, Q. Paracrine mechanisms of mesenchymal stem cell-based therapy: Current status and perspectives. *Cell Transplant.* **2014**, *23*, 1045–1059. [CrossRef]
32. Xu, P.; Yang, X. The efficacy and safety of mesenchymal stem cell transplantation for spinal cord injury patients: A meta-analysis and systematic review. *Cell Transplant.* **2019**, *28*, 36–46. [CrossRef]
33. Connick, P.; Kolappan, M.; Crawley, C.; Webber, D.J.; Patani, R.; Michell, A.W.; Du, M.-Q.; Luan, S.-L.; Altmann, D.R.; Thompson, A.J. Autologous mesenchymal stem cells for the treatment of secondary progressive multiple sclerosis: An open-label phase 2a proof-of-concept study. *Lancet Neurol.* **2012**, *11*, 150–156. [CrossRef]
34. Lee, J.S.; Hong, J.M.; Moon, G.J.; Lee, P.H.; Ahn, Y.H.; Bang, O.Y. A long-term follow-up study of intravenous autologous mesenchymal stem cell transplantation in patients with ischemic stroke. *Stem Cells* **2010**, *28*, 1099–1106. [CrossRef]
35. Gupta, P.K.; Das, A.K.; Chullikana, A.; Majumdar, A.S. Mesenchymal stem cells for cartilage repair in osteoarthritis. *Stem Cell Res. Ther.* **2012**, *3*, 25. [CrossRef]
36. Wang, L.; Wang, L.; Cong, X.; Liu, G.; Zhou, J.; Bai, B.; Li, Y.; Bai, W.; Li, M.; Ji, H. Human umbilical cord mesenchymal stem cell therapy for patients with active rheumatoid arthritis: Safety and efficacy. *Stem Cells Dev.* **2013**, *22*, 3192–3202. [CrossRef]
37. Chou, S.-H.; Lin, S.-Z.; Kuo, W.-W.; Pai, P.; Lin, J.-Y.; Lai, C.-H.; Kuo, C.-H.; Lin, K.-H.; Tsai, F.-J.; Huang, C.-Y. Mesenchymal stem cell insights: Prospects in cardiovascular therapy. *Cell Transplant.* **2014**, *23*, 513–529. [CrossRef]
38. Tögel, F.; Westenfelder, C. Adult bone marrow–derived stem cells for organ regeneration and repair. *Dev. Dyn.* **2007**, *236*, 3321–3331. [CrossRef]
39. Ide, C.; Nakai, Y.; Nakano, N.; Seo, T.-B.; Yamada, Y.; Endo, K.; Noda, T.; Saito, F.; Suzuki, Y.; Fukushima, M. Bone marrow stromal cell transplantation for treatment of sub-acute spinal cord injury in the rat. *Brain Res.* **2010**, *1332*, 32–47. [CrossRef]
40. Chimenti, I.; Smith, R.R.; Li, T.-S.; Gerstenblith, G.; Messina, E.; Giacomello, A.; Marbán, E. Relative roles of direct regeneration versus paracrine effects of human cardiosphere-derived cells transplanted into infarcted mice. *Circ. Res.* **2010**, *106*, 971–980. [CrossRef]
41. Park, W.S.; Ahn, S.Y.; Sung, S.I.; Ahn, J.-Y.; Chang, Y.S. Strategies to enhance paracrine potency of transplanted mesenchymal stem cells in intractable neonatal disorders. *Pediatr. Res.* **2018**, *83*, 214–222. [CrossRef] [PubMed]
42. Vizoso, F.J.; Eiro, N.; Cid, S.; Schneider, J.; Perez-Fernandez, R. Mesenchymal stem cell secretome: Toward cell-free therapeutic strategies in regenerative medicine. *Int. J. Mol. Sci.* **2017**, *18*, 1852. [CrossRef] [PubMed]
43. Wang, S.; Qu, X.; Zhao, R.C. Clinical applications of mesenchymal stem cells. *J. Hematol. Oncol.* **2012**, *5*, 1–9. [CrossRef]
44. Zhou, T.; Yuan, Z.; Weng, J.; Pei, D.; Du, X.; He, C.; Lai, P. Challenges and advances in clinical applications of mesenchymal stromal cells. *J. Hematol. Oncol.* **2021**, *14*, 24. [CrossRef]
45. Phinney, D.G.; Kopen, G.; Righter, W.; Webster, S.; Tremain, N.; Prockop, D.J. Donor variation in the growth properties and osteogenic potential of human marrow stromal cells. *J. Cell. Biochem.* **1999**, *75*, 424–436. [CrossRef]
46. McLeod, C.; Mauck, R. On the origin and impact of mesenchymal stem cell heterogeneity: New insights and emerging tools for single cell analysis. *Eur. Cells Mater.* **2017**, *34*, 217. [CrossRef]
47. Ryan, A.E.; Lohan, P.; O'flynn, L.; Treacy, O.; Chen, X.; Coleman, C.; Shaw, G.; Murphy, M.; Barry, F.; Griffin, M.D. Chondrogenic differentiation increases antidonor immune response to allogeneic mesenchymal stem cell transplantation. *Mol. Ther.* **2014**, *22*, 655–667. [CrossRef]

48. Nicolay, N.H.; Perez, R.L.; Debus, J.; Huber, P.E. Mesenchymal stem cells—A new hope for radiotherapy-induced tissue damage? *Cancer Lett.* **2015**, *366*, 133–140. [CrossRef]
49. Costa, L.A.; Eiro, N.; Fraile, M.; Gonzalez, L.O.; Saá, J.; Garcia-Portabella, P.; Vega, B.; Schneider, J.; Vizoso, F.J. Functional heterogeneity of mesenchymal stem cells from natural niches to culture conditions: Implications for further clinical uses. *Cell. Mol. Life Sci.* **2021**, *78*, 447–467. [CrossRef]
50. Herberts, C.A.; Kwa, M.S.; Hermsen, H.P. Risk factors in the development of stem cell therapy. *J. Transl. Med.* **2011**, *9*, 29. [CrossRef]
51. Drela, K.; Stanaszek, L.; Nowakowski, A.; Kuczynska, Z.; Lukomska, B. Experimental strategies of mesenchymal stem cell propagation: Adverse events and potential risk of functional changes. *Stem Cells Int.* **2019**, *2019*, 7012692. [CrossRef]
52. Suhito, I.R.; Han, Y.; Min, J.; Son, H.; Kim, T.-H. In situ label-free monitoring of human adipose-derived mesenchymal stem cell differentiation into multiple lineages. *Biomaterials* **2018**, *154*, 223–233. [CrossRef]
53. Lee, J.; Cha, H.; Park, T.H.; Park, J.H. Enhanced osteogenic differentiation of human mesenchymal stem cells by direct delivery of Cbfβ protein. *Biotechnol. Bioeng.* **2020**, *117*, 2897–2910. [CrossRef]
54. Honarpardaz, A.; Irani, S.; Pezeshki-Modaress, M.; Zandi, M.; Sadeghi, A. Enhanced chondrogenic differentiation of bone marrow mesenchymal stem cells on gelatin/glycosaminoglycan electrospun nanofibers with different amount of glycosaminoglycan. *J. Biomed. Mater. Res. A* **2019**, *107*, 38–48. [CrossRef]
55. Yoon, H.H.; Bhang, S.H.; Kim, T.; Yu, T.; Hyeon, T.; Kim, B.S. Dual roles of graphene oxide in chondrogenic differentiation of adult stem cells: Cell-adhesion substrate and growth factor-delivery carrier. *Adv. Funct. Mater.* **2014**, *24*, 6455–6464. [CrossRef]
56. Thomson, J.A.; Itskovitz-Eldor, J.; Shapiro, S.S.; Waknitz, M.A.; Swiergiel, J.J.; Marshall, V.S.; Jones, J.M. Embryonic stem cell lines derived from human blastocysts. *Science* **1998**, *282*, 1145–1147. [CrossRef]
57. Yamanaka, S. Pluripotent stem cell-based cell therapy—Promise and challenges. *Cell Stem Cell* **2020**, *27*, 523–531. [CrossRef]
58. Takahashi, K.; Yamanaka, S. Induction of pluripotent stem cells from mouse embryonic and adult fibroblast cultures by defined factors. *Cell* **2006**, *126*, 663–676. [CrossRef]
59. Seki, T.; Fukuda, K. Methods of induced pluripotent stem cells for clinical application. *World J. Stem Cells* **2015**, *7*, 116. [CrossRef]
60. Baker, M. Why hES cells make teratomas. *Nat. Rep. Stem Cells* **2009**. [CrossRef]
61. Nishizawa, M.; Chonabayashi, K.; Nomura, M.; Tanaka, A.; Nakamura, M.; Inagaki, A.; Nishikawa, M.; Takei, I.; Oishi, A.; Tanabe, K.; et al. Epigenetic variation between human induced pluripotent stem cell lines is an indicator of differentiation capacity. *Cell Stem Cell* **2016**, *19*, 341–354. [CrossRef] [PubMed]
62. Hayashi, R.; Ishikawa, Y.; Katori, R.; Sasamoto, Y.; Taniwaki, Y.; Takayanagi, H.; Tsujikawa, M.; Sekiguchi, K.; Quantock, A.J.; Nishida, K. Coordinated generation of multiple ocular-like cell lineages and fabrication of functional corneal epithelial cell sheets from human iPS cells. *Nat. Protoc.* **2017**, *12*, 683–696. [CrossRef] [PubMed]
63. Hayashi, R.; Ishikawa, Y.; Katayama, T.; Quantock, A.J.; Nishida, K. CD200 facilitates the isolation of corneal epithelial cells derived from human pluripotent stem cells. *Sci. Rep.* **2018**, *8*, 16550. [CrossRef] [PubMed]
64. Tang, F.; Barbacioru, C.; Wang, Y.; Nordman, E.; Lee, C.; Xu, N.; Wang, X.; Bodeau, J.; Tuch, B.B.; Siddiqui, A. mRNA-Seq whole-transcriptome analysis of a single cell. *Nat. Methods* **2009**, *6*, 377–382. [CrossRef]
65. Sun, C.; Wang, L.; Wang, H.; Huang, T.; Yao, W.; Li, J.; Zhang, X. Single-cell RNA-seq highlights heterogeneity in human primary Wharton's jelly mesenchymal stem/stromal cells cultured in vitro. *Stem Cell Res. Ther.* **2020**, *11*, 149. [CrossRef]
66. Camp, J.G.; Wollny, D.; Treutlein, B. Single-cell genomics to guide human stem cell and tissue engineering. *Nat. Methods* **2018**, *15*, 661–667. [CrossRef]
67. Chu, L.-F.; Leng, N.; Zhang, J.; Hou, Z.; Mamott, D.; Vereide, D.T.; Choi, J.; Kendziorski, C.; Stewart, R.; Thomson, J.A. Single-cell RNA-seq reveals novel regulators of human embryonic stem cell differentiation to definitive endoderm. *Genome Biol.* **2016**, *17*, 173. [CrossRef]
68. Kee, N.; Volakakis, N.; Kirkeby, A.; Dahl, L.; Storvall, H.; Nolbrant, S.; Lahti, L.; Björklund, Å.K.; Gillberg, L.; Joodmardi, E.; et al. Single-cell analysis reveals a close relationship between differentiating dopamine and subthalamic nucleus neuronal lineages. *Cell Stem Cell* **2017**, *20*, 29–40. [CrossRef]
69. Yao, Z.; Mich, J.K.; Ku, S.; Menon, V.; Krostag, A.-R.; Martinez, R.A.; Furchtgott, L.; Mulholland, H.; Bort, S.; Fuqua, M.A.; et al. A single-cell roadmap of lineage bifurcation in human ESC models of embryonic brain development. *Cell Stem Cell* **2017**, *20*, 120–134. [CrossRef]
70. Kebschull, J.M.; Zador, A.M. Cellular barcoding: Lineage tracing, screening and beyond. *Nat. Methods* **2018**, *15*, 871–879. [CrossRef]
71. Kester, L.; van Oudenaarden, A. Single-cell transcriptomics meets lineage tracing. *Cell Stem Cell* **2018**, *23*, 166–179. [CrossRef]
72. Weinreb, C.; Klein, A.M. Lineage reconstruction from clonal correlations. *Proc. Natl. Acad. Sci. USA.* **2020**, *117*, 17041–17048. [CrossRef]
73. Biddy, B.A.; Kong, W.; Kamimoto, K.; Guo, C.; Waye, S.E.; Sun, T.; Morris, S.A. Single-cell mapping of lineage and identity in direct reprogramming. *Nature* **2018**, *564*, 219–224. [CrossRef]
74. Pei, W.; Feyerabend, T.B.; Rössler, J.; Wang, X.; Postrach, D.; Busch, K.; Rode, I.; Klapproth, K.; Dietlein, N.; Quedenau, C.; et al. Polylox barcoding reveals haematopoietic stem cell fates realized in vivo. *Nature* **2017**, *548*, 456–460. [CrossRef]
75. Weinreb, C.; Rodriguez-Fraticelli, A.; Camargo, F.D.; Klein, A.M. Lineage tracing on transcriptional landscapes links state to fate during differentiation. *Science* **2020**, *367*, eaaw3381. [CrossRef]

76. Loulier, K.; Barry, R.; Mahou, P.; Le Franc, Y.; Supatto, W.; Matho, K.S.; Ieng, S.; Fouquet, S.; Dupin, E.; Benosman, R. Multiplex cell and lineage tracking with combinatorial labels. *Neuron* **2014**, *81*, 505–520. [CrossRef]
77. Jinek, M.; Chylinski, K.; Fonfara, I.; Hauer, M.; Doudna, J.A.; Charpentier, E. A programmable dual-RNA-guided DNA endonuclease in adaptive bacterial immunity. *Science* **2012**, *337*, 816–821. [CrossRef]
78. Kalhor, R.; Mali, P.; Church, G.M. Rapidly evolving homing CRISPR barcodes. *Nat. Methods* **2017**, *14*, 195–200. [CrossRef]
79. Strzelecka, P.M.; Ranzoni, A.M.; Cvejic, A. Dissecting human disease with single-cell omics: Application in model systems and in the clinic. *Dis. Model Mech.* **2018**, *11*, dmm036525. [CrossRef]
80. Paik, D.T.; Cho, S.; Tian, L.; Chang, H.Y.; Wu, J.C. Single-cell RNA sequencing in cardiovascular development, disease and medicine. *Nat. Rev. Cardiol.* **2020**, *17*, 457–473. [CrossRef]
81. Morris, S.A. The evolving concept of cell identity in the single cell era. *Development* **2019**, *146*, dev169748. [CrossRef] [PubMed]
82. Lin, X.; Liu, H.; Wei, Z.; Roy, S.B.; Gao, N. An active learning approach for clustering single-cell RNA-seq data. *Lab. Investig.* **2022**, *102*, 227–235. [CrossRef] [PubMed]
83. Kong, W.; Biddy, B.A.; Kamimoto, K.; Amrute, J.M.; Butka, E.G.; Morris, S.A. CellTagging: Combinatorial indexing to simultaneously map lineage and identity at single-cell resolution. *Nat. Protoc.* **2020**, *15*, 750–772. [CrossRef] [PubMed]
84. Wagner, D.E.; Klein, A.M. Lineage tracing meets single-cell omics: Opportunities and challenges. *Nat. Rev. Genet.* **2020**, *21*, 410–427. [CrossRef]
85. Specht, E.A.; Braselmann, E.; Palmer, A.E. A critical and comparative review of fluorescent tools for live-cell imaging. *Annu. Rev. Physiol.* **2017**, *79*, 93–117. [CrossRef]
86. Tsien, R.Y.; Ernst, L.; Waggoner, A. Fluorophores for confocal microscopy: Photophysics and photochemistry. In *Handbook of Biological Confocal Microscopy*; Pawley, J.B., Ed.; Springer: Boston, MA, USA, 2006; pp. 338–352.
87. Meng, F.; Wang, J.; Ping, Q.; Yeo, Y. Quantitative assessment of nanoparticle biodistribution by fluorescence imaging, revisited. *ACS Nano* **2018**, *12*, 6458–6468. [CrossRef]
88. Cox, G. *Fundamentals of Fluorescence Imaging*; CRC Press: Boca Raton, FL, USA, 2019.
89. Rao, J.; Dragulescu-Andrasi, A.; Yao, H. Fluorescence imaging in vivo: Recent advances. *Curr. Opin. Biotechnol.* **2007**, *18*, 17–25. [CrossRef]
90. Thorp-Greenwood, F.L. An introduction to organometallic complexes in fluorescence cell imaging: Current applications and future prospects. *Organometallics* **2012**, *31*, 5686–5692. [CrossRef]
91. Flanagan, L.A.; Ziaeian, B.; Palmer, T.; Schwartz, P.H. CHAPTER 9-Immunocytochemical analysis of stem cells. In *Human Stem Cell Manual*; Loring, J.F., Wesselschmidt, R.L., Schwartz, P.H., Eds.; Academic Press: Oxford, UK, 2007; pp. 108–126.
92. Van Hoof, D.; Passier, R.; Ward-Van Oostwaard, D.; Pinkse, M.W.; Heck, A.J.; Mummery, C.L.; Krijgsveld, J. A quest for human and mouse embryonic stem cell-specific proteins* S. *Mol. Cell. Proteom.* **2006**, *5*, 1261–1273. [CrossRef]
93. Fong, C.Y.; Peh, G.S.; Gauthaman, K.; Bongso, A. Separation of SSEA-4 and TRA-1–60 labelled undifferentiated human embryonic stem cells from a heterogeneous cell population using magnetic-activated cell sorting (MACS) and fluorescence-activated cell sorting (FACS). *Stem Cell Rev. Rep.* **2009**, *5*, 72–80. [CrossRef]
94. Brivanlou, A.H.; Gage, F.H.; Jaenisch, R.; Jessell, T.; Melton, D.; Rossant, J. Setting standards for human embryonic stem cells. *Science* **2003**, *300*, 913–916. [CrossRef]
95. Abe, R.; Yamauchi, K.; Kuniyoshi, K.; Suzuki, T.; Matsuura, Y.; Ohtori, S.; Takahashi, K. Neural crest stem cells can be induced in vitro from human-induced pluripotent stem cells using a novel protocol free of feeder cells. *J. Rural Med.* **2021**, *16*, 143–147. [CrossRef]
96. Niwa, H.; Miyazaki, J.-I.; Smith, A.G. Quantitative expression of Oct-3/4 defines differentiation, dedifferentiation or self-renewal of ES cells. *Nature Genet.* **2000**, *24*, 372–376. [CrossRef]
97. Yuan, H.; Corbi, N.; Basilico, C.; Dailey, L. Developmental-specific activity of the FGF-4 enhancer requires the synergistic action of Sox2 and Oct-3. *Genes Dev.* **1995**, *9*, 2635–2645. [CrossRef]
98. Bredenkamp, N.; Stirparo, G.G.; Nichols, J.; Smith, A.; Guo, G. The cell-surface marker sushi containing domain 2 facilitates establishment of human naive pluripotent stem cells. *Stem Cell Rep.* **2019**, *12*, 1212–1222. [CrossRef]
99. Yuan, H.; Hu, H.; Chen, R.; Mu, W.; Wang, L.; Li, Y.; Chen, Y.; Ding, X.; Xi, Y.; Mao, S. Premigratory neural crest stem cells generate enteric neurons populating the mouse colon and regulating peristalsis in tissue-engineered intestine. *Stem Cells Trans. Med.* **2021**, *10*, 922–938. [CrossRef]
100. Tian, Y.I.; Zhang, X.; Torrejon, K.; Danias, J.; Gindina, S.; Nayyar, A.; Du, Y.; Xie, Y. A bioengineering approach to Schlemm's canal-like stem cell differentiation for in vitro glaucoma drug screening. *Acta Biomater.* **2020**, *105*, 203–213. [CrossRef]
101. Darvishi, M.; Hamidabadi, H.G.; Bojnordi, M.N.; Zahiri, M.; Niapour, A.; Alizadeh, R. Differentiation of human dental pulp stem cells into functional motor neuron: In vitro and ex vivo study. *Tissue Cell* **2021**, *72*, 101542. [CrossRef]
102. Yang, X.; Han, G.; Pang, X.; Fan, M. Chitosan/collagen scaffold containing bone morphogenetic protein-7 DNA supports dental pulp stem cell differentiation in vitro and in vivo. *J. Biomed. Mater. Res. A* **2020**, *108*, 2519–2526. [CrossRef]
103. Okajcekova, T.; Strnadel, J.; Pokusa, M.; Zahumenska, R.; Janickova, M.; Halasova, E.; Skovierova, H. A comparative in vitro analysis of the osteogenic potential of human dental pulp stem cells using various differentiation conditions. *Int. J. Mol. Sci.* **2020**, *21*, 2280. [CrossRef]

104. Perczel-Kovách, K.; Hegedűs, O.; Földes, A.; Sangngoen, T.; Kálló, K.; Steward, M.C.; Varga, G.; Nagy, K.S. STRO-1 positive cell expansion during osteogenic differentiation: A comparative study of three mesenchymal stem cell types of dental origin. *Arch. Oral Biol.* **2021**, *122*, 104995. [CrossRef]
105. Mennen, R.H.G.; Pennings, J.L.A.J.; Piersma, A.H.A. Neural crest related gene transcript regulation by valproic acid analogues in the cardiac embryonic stem cell test. *Reprod. Toxicol.* **2019**, *90*, 44–52. [CrossRef]
106. Zhang, S.; Hang, Y.; Wu, J.; Tang, Z.; Li, X.; Zhang, S.; Wang, L.; Brash, J.L.; Chen, H. Dual pathway for promotion of stem cell neural differentiation mediated by gold nanocomposites. *ACS Appl. Mater. Interfaces* **2020**, *12*, 22066–22073. [CrossRef]
107. Ku, T.; Hao, F.; Yang, X.; Rao, Z.; Liu, Q.S.; Sang, N.; Faiola, F.; Zhou, Q.; Jiang, G. Graphene quantum dots disrupt embryonic stem cell differentiation by interfering with the methylation level of Sox2. *Environ. Sci. Technol.* **2021**, *55*, 3144–3155. [CrossRef]
108. Regent, F.; Morizur, L.; Lesueur, L.; Habeler, W.; Plancheron, A.; Ben M'Barek, K.; Monville, C. Automation of human pluripotent stem cell differentiation toward retinal pigment epithelial cells for large-scale productions. *Sci. Rep.* **2019**, *9*, 10646. [CrossRef]
109. Duong, A.; Evstratova, A.; Sivitilli, A.; Hernandez, J.J.; Gosio, J.; Wahedi, A.; Sondheimer, N.; Wrana, J.L.; Beaulieu, J.-M.; Attisano, L. Characterization of mitochondrial health from human peripheral blood mononuclear cells to cerebral organoids derived from induced pluripotent stem cells. *Sci. Rep.* **2021**, *11*, 4523. [CrossRef]
110. Chen, C.X.Q.; Abdian, N.; Maussion, G.; Thomas, R.A.; Demirova, I.; Cai, E.; Tabatabaei, M.; Beitel, L.K.; Karamchandani, J.; Fon, E.A.; et al. Standardized quality control workflow to evaluate the reproducibility and differentiation potential of human iPSCs into neurons. *bioRxiv* **2021**. [CrossRef]
111. Urrutia-Cabrera, D.; Hsiang-Chi Liou, R.; Lin, J.; Shi, Y.; Liu, K.; Hung, S.S.C.; Hewitt, A.W.; Wang, P.-Y.; Ching-Bong Wong, R. Combinatorial approach of binary colloidal crystals and CRISPR activation to improve induced pluripotent stem cell differentiation into neurons. *ACS Appl. Mater. Interfaces* **2022**, *14*, 8669–8679. [CrossRef]
112. Kobolak, J.; Teglasi, A.; Bellak, T.; Janstova, Z.; Molnar, K.; Zana, M.; Bock, I.; Laszlo, L.; Dinnyes, A. Human induced pluripotent stem cell-derived 3D-neurospheres are suitable for neurotoxicity screening. *Cells* **2020**, *9*, 1122. [CrossRef]
113. Lee, Y.; Choi, H.Y.; Kwon, A.; Park, H.; Park, M.-H.; Kim, J.-W.; Kim, M.J.; Kim, Y.-O.; Kwak, S.; Koo, S.K. Generation of a PDX1–EGFP reporter human induced pluripotent stem cell line, KSCBi005-A-3, using the CRISPR/Cas9 system. *Stem Cell Res.* **2019**, *41*, 101632. [CrossRef]
114. Fleischer, S.; Jahnke, H.-G.; Fritsche, E.; Girard, M.; Robitzki, A.A. Comprehensive human stem cell differentiation in a 2D and 3D mode to cardiomyocytes for long-term cultivation and multiparametric monitoring on a multimodal microelectrode array setup. *Biosens. Bioelectron.* **2019**, *126*, 624–631. [CrossRef] [PubMed]
115. Suryawan, I.G.R.; Andrianto; Anggaraeni, A.D.; Agita, A.; Nugraha, R.A. The role of human platelet-rich plasma to enhance the differentiation from adipose derived mesenchymal stem cells into cardiomyocyte: An experimental study. *bioRxiv* **2021**. [CrossRef]
116. Chang, Y.-H.; Kumar, V.B.; Wen, Y.-T.; Huang, C.-Y.; Tsai, R.-K.; Ding, D.-C. Induction of human umbilical mesenchymal stem cell differentiation into retinal pigment epithelial cells using atranswell-based co-culture system. *Cell Transplat.* **2022**, *31*, 09636897221085901. [CrossRef] [PubMed]
117. Ekram, S.; Khalid, S.; Bashir, I.; Salim, A.; Khan, I. Human umbilical cord-derived mesenchymal stem cells and their chondroprogenitor derivatives reduced pain and inflammation signaling and promote regeneration in a rat intervertebral disc degeneration model. *Mol. Cell. Biochem.* **2021**, *476*, 3191–3205. [CrossRef]
118. Wu, S.-H.; Liao, Y.-T.; Hsueh, K.-K.; Huang, H.-K.; Chen, T.-M.; Chiang, E.-R.; Hsu, S.-H.; Tseng, T.-C.; Wang, J.-P. Adipose-derived mesenchymal stem cells from a hypoxic culture improve neuronal differentiation and nerve repair. *Front. Cell. Dev. Biol.* **2021**, *9*, 1110. [CrossRef]
119. Swanson, W.B.; Omi, M.; Zhang, Z.; Nam, H.K.; Jung, Y.; Wang, G.; Ma, P.X.; Hatch, N.E.; Mishina, Y. Macropore design of tissue engineering scaffolds regulates mesenchymal stem cell differentiation fate. *Biomaterials* **2021**, *272*, 120769. [CrossRef]
120. Kadkhodaeian, H.A.; Salati, A.; Ansari, M.; Nooshabadi, V.T. Tracking the transplanted neurosphere in retinal pigment epithelium degeneration model. *Basic Clin. Neurosci.* **2021**, *12*, 523. [CrossRef]
121. Yu, M.; Lei, B.; Gao, C.; Yan, J.; Ma, P.X. Optimizing surface-engineered ultra-small gold nanoparticles for highly efficient miRNA delivery to enhance osteogenic differentiation of bone mesenchymal stromal cells. *Nano Res.* **2017**, *10*, 49–63. [CrossRef]
122. Niu, Y.-T.; Xie, L.; Deng, R.-R.; Zhang, X.-Y. In the presence of TGF-β1, Asperosaponin VI promotes human mesenchymal stem cell differentiation into nucleus pulposus like- cells. *BMC Complement. Med. Ther.* **2021**, *21*, 32. [CrossRef]
123. Dadheech, N.; Srivastava, A.; Vakani, M.; Shrimali, P.; Bhonde, R.; Gupta, S. Direct lineage tracing reveals Activin—A potential for improved pancreatic homing of bone marrow mesenchymal stem cells and efficient ß-cell regeneration in vivo. *Stem Cell Res.* **2020**, *11*, 327. [CrossRef]
124. Ojaghi, M.; Soleimanifar, F.; Kazemi, A.; Ghollasi, M.; Soleimani, M.; Nasoohi, N.; Enderami, S.E. Electrospun poly-l-lactic acid/polyvinyl alcohol nanofibers improved insulin-producing cell differentiation potential of human adipose-derived mesenchymal stem cells. *J. Cell. Biochem.* **2019**, *120*, 9917–9926. [CrossRef]
125. Patil, S.; Singh, N. Silk fibroin-alginate based beads for human mesenchymal stem cell differentiation in 3D. *Biomater. Sci.* **2019**, *7*, 4687–4697. [CrossRef]
126. Sokolowska, P.; Zukowski, K.; Lasocka, I.; Szulc-Dabrowska, L.; Jastrzebska, E. Human mesenchymal stem cell (hMSC) differentiation towards cardiac cells using a new microbioanalytical method. *Analyst* **2020**, *145*, 3017–3028. [CrossRef]

127. Parodi, V.; Jacchetti, E.; Bresci, A.; Talone, B.; Valensise, C.M.; Osellame, R.; Cerullo, G.; Polli, D.; Raimondi, M.T. Characterization of mesenchymal stem cell differentiation within miniaturized 3D scaffolds through advanced microscopy techniques. *Int. J. Mol. Sci.* **2020**, *21*, 8498. [CrossRef]
128. Sharma, K.D.; Alghazali, K.M.; Hamzah, R.N.; Pandanaboina, S.C.; Nima Alsudani, Z.A.; Muhi, M.; Watanabe, F.; Zhou, G.-L.; Biris, A.S.; Xie, J.Y. Gold nanorod substrate for rat fetal neural stem cell differentiation into oligodendrocytes. *Nanomaterials* **2022**, *12*, 929. [CrossRef]
129. Qu, A.; Sun, M.; Kim, J.-Y.; Xu, L.; Hao, C.; Ma, W.; Wu, X.; Liu, X.; Kuang, H.; Kotov, N.A. Stimulation of neural stem cell differentiation by circularly polarized light transduced by chiral nanoassemblies. *Nat. Biomed. Eng.* **2021**, *5*, 103–113. [CrossRef]
130. Menéndez-Méndez, A.; Paniagua-Herranz, L.; Olivos-Oré, L.A.; Gómez-Villafuertes, R.; Pérez-Sen, R.; Delicado, E.G.; Artalejo, A.R.; Ortega, F. Combining low-density cell culture, single-cell tracking, and patch-clamp to monitor the behavior of postnatal murine cerebellar neural stem cells. *STAR Protoc.* **2021**, *2*, 100964. [CrossRef]
131. Zhang, C.; Tu, H.-L.; Jia, G.; Mukhtar, T.; Taylor, V.; Rzhetsky, A.; Tay, S. Ultra-multiplexed analysis of single-cell dynamics reveals logic rules in differentiation. *Sci. Adv.* **2019**, *5*, eaav7959. [CrossRef]
132. Jaberi, R.; Mirsadeghi, S.; Kiani, S. In vitro characterization of subventricular zone isolated neural stem cells, from adult monkey and rat brain. *Mol. Biol. Rep.* **2021**, *48*, 1311–1321. [CrossRef]
133. Jung, S.; Harris, N.; Niyonshuti, I.I.; Jenkins, S.V.; Hayar, A.M.; Watanabe, F.; Jamshidi-Parsian, A.; Chen, J.; Borrelli, M.J.; Griffin, R.J. Photothermal response induced by nanocage-coated artificial extracellular matrix promotes neural stem cell differentiation. *Nanomaterials* **2021**, *11*, 1216. [CrossRef]
134. Marchini, A.; Favoino, C.; Gelain, F. Multi-functionalized self-assembling peptides as reproducible 3D cell culture systems enabling differentiation and survival of various human neural stem cell lines. *Front. Neurosci.* **2020**, *14*, 413. [CrossRef]
135. Lee, I.C.; Wu, H.J.; Liu, H.L. Dual-frequency ultrasound induces neural stem/progenitor cell differentiation and growth factor utilization by enhancing stable cavitation. *ACS Chem. Neurosci.* **2019**, *10*, 1452–1461. [CrossRef]
136. Sui, Y.; Zhang, W.; Tang, T.; Gao, L.; Cao, T.; Zhu, H.; You, Q.; Yu, B.; Yang, T. Insulin-like growth factor-II overexpression accelerates parthenogenetic stem cell differentiation into cardiomyocytes and improves cardiac function after acute myocardial infarction in mice. *Stem Cell Res. Ther.* **2020**, *11*, 86. [CrossRef] [PubMed]
137. Zhong, W. Nanomaterials in fluorescence-based biosensing. *Anal. Bioanal. Chem.* **2009**, *394*, 47–59. [CrossRef] [PubMed]
138. Kim, J.; Song, S.H.; Jin, Y.; Park, H.-J.; Yoon, H.; Jeon, S.; Cho, S.-W. Multiphoton luminescent graphene quantum dots for in vivo tracking of human adipose-derived stem cells. *Nanoscale* **2016**, *8*, 8512–8519. [CrossRef] [PubMed]
139. Niaraki, A.; Shirsavar, M.A.; Aykar, S.S.; Taghavimehr, M.; Montazami, R.; Hashemi, N.N. Minute-sensitive real-time monitoring of neural cells through printed graphene microelectrodes. *Biosens. Bioelectron.* **2022**, *210*, 114284. [CrossRef] [PubMed]
140. Ji, Y.; Li, Y.-M.; Seo, J.G.; Jang, T.-S.; Knowles, J.C.; Song, S.H.; Lee, J.-H. Biological potential of polyethylene glycol (PEG)-functionalized graphene quantum dots in in vitro neural stem/progenitor cells. *Nanomaterials* **2021**, *11*, 1446. [CrossRef] [PubMed]
141. Liu, S.; Tay, L.M.; Anggara, R.; Chuah, Y.J.; Kang, Y. Long-term tracking mesenchymal stem cell differentiation with photostable fluorescent nanoparticles. *ACS Appl. Mater. Interfaces* **2016**, *8*, 11925–11933. [CrossRef]
142. Wang, L.; Xu, K.; Hou, X.; Han, Y.; Liu, S.; Wiraja, C.; Yang, C.; Yang, J.; Wang, M.; Dong, X. Fluorescent poly (glycerol-co-sebacate) acrylate nanoparticles for stem cell labeling and longitudinal tracking. *ACS Appl. Mater. Interfaces* **2017**, *9*, 9528–9538. [CrossRef]
143. Jang, S.E.; Qiu, L.; Cai, X.; Lee, J.W.L.; Zhang, W.; Tan, E.-K.; Liu, B.; Zeng, L. Aggregation-induced emission (AIE) nanoparticles labeled human embryonic stem cells (hESCs)-derived neurons for transplantation. *Biomaterials* **2021**, *271*, 120747. [CrossRef]
144. Choi, C.K.K.; Li, J.; Wei, K.; Xu, Y.J.; Ho, L.W.C.; Zhu, M.; To, K.K.; Choi, C.H.J.; Bian, L. A gold@ polydopamine core–shell nanoprobe for long-term intracellular detection of microRNAs in differentiating stem cells. *J. Am. Chem. Soc.* **2015**, *137*, 7337–7346. [CrossRef]
145. Yue, S.; Li, Y.; Qiao, Z.; Song, W.; Bi, S. Rolling circle replication for biosensing, bioimaging, and biomedicine. *Trends Biotechnol.* **2021**, *39*, 1160–1172. [CrossRef]
146. Shi, P.; Wang, Y. Synthetic DNA for cell-surface engineering. *Angew. Chem. Int. Ed.* **2021**, *133*, 11684–11695. [CrossRef]
147. Bi, S.; Yue, S.; Zhang, S. Hybridization chain reaction: A versatile molecular tool for biosensing, bioimaging, and biomedicine. *Chem. Soc. Rev.* **2017**, *46*, 4281–4298. [CrossRef]
148. Samia, A.C.; Chen, X.; Burda, C. Semiconductor quantum dots for photodynamic therapy. *J. Am. Chem. Soc.* **2003**, *125*, 15736–15737. [CrossRef]
149. Zhang, X.; Wang, S.; Xu, L.; Feng, L.; Ji, Y.; Tao, L.; Li, S.; Wei, Y. Biocompatible polydopamine fluorescent organic nanoparticles: Facile preparation and cell imaging. *Nanoscale* **2012**, *4*, 5581–5584. [CrossRef]
150. Li, X.; Que, L. Fluorescence enhancement enabled by nanomaterials and nanostructured substrates: A brief review. *Rev. Nanosci. Nanotechnol.* **2014**, *3*, 161–176. [CrossRef]
151. Li, J.; Leung, C.W.T.; Wong, D.S.H.; Xu, J.; Li, R.; Zhao, Y.; Yung, C.Y.Y.; Zhao, E.; Tang, B.Z.; Bian, L. Photocontrolled siRNA delivery and biomarker-triggered luminogens of aggregation-induced emission by up-conversion $NaYF_4$:$Yb^{3+}Tm^{3+}$@SiO_2 nanoparticles for inducing and monitoring stem-cell differentiation. *ACS Appl. Mater. Interfaces* **2019**, *11*, 22074–22084. [CrossRef]
152. Sharifi, M.; Attar, F.; Saboury, A.A.; Akhtari, K.; Hooshmand, N.; Hasan, A.; El-Sayed, M.A.; Falahati, M. Plasmonic gold nanoparticles: Optical manipulation, imaging, drug delivery and therapy. *J. Control. Release* **2019**, *311–312*, 170–189. [CrossRef]

153. Wu, Q.; Wang, K.; Wang, X.; Liang, G.; Li, J. Delivering siRNA to control osteogenic differentiation and real-time detection of cell differentiation in human mesenchymal stem cells using multifunctional gold nanoparticles. *J. Mat. Chem. B* **2020**, *8*, 3016–3027. [CrossRef]
154. Palonpon, A.F.; Sodeoka, M.; Fujita, K. Molecular imaging of live cells by Raman microscopy. *Curr. Opin. Chem. Biol.* **2013**, *17*, 708–715. [CrossRef] [PubMed]
155. Chan, J.W.; Lieu, D.K. Label-free biochemical characterization of stem cells using vibrational spectroscopy. *J. Biophotonics* **2009**, *2*, 656–668. [CrossRef] [PubMed]
156. Ghita, A.; Pascut, F.C.; Sottile, V.; Denning, C.; Notingher, I. Applications of Raman micro-spectroscopy to stem cell technology: Label-free molecular discrimination and monitoring cell differentiation. *EPJ Tech. Instrum.* **2015**, *2*, 1–14. [CrossRef] [PubMed]
157. Sil, S.; Mukherjee, R.; Kumbhar, D.; Reghu, D.; Shrungar, D.; Kumar, N.S.; Singh, U.K.; Umapathy, S. Raman spectroscopy and artificial intelligence open up accurate detection of pathogens from DNA-based sub-species level classification. *J. Raman Spectrosc.* **2021**, *52*, 2648–2659. [CrossRef]
158. Camp, C.H., Jr.; Cicerone, M.T. Chemically sensitive bioimaging with coherent Raman scattering. *Nat. Photonics* **2015**, *9*, 295–305. [CrossRef]
159. Smith, R.; Wright, K.L.; Ashton, L. Raman spectroscopy: An evolving technique for live cell studies. *Analyst* **2016**, *141*, 3590–3600. [CrossRef]
160. Pan, L.; Zhang, P.; Daengngam, C.; Peng, S.; Chongcheawchamnan, M. A review of artificial intelligence methods combined with Raman spectroscopy to identify the composition of substances. *J. Raman Spectrosc.* **2022**, *53*, 6–19. [CrossRef]
161. Liu, Z.; Guo, Z.; Zhong, H.; Qin, X.; Wan, M.; Yang, B. Graphene oxide based surface-enhanced Raman scattering probes for cancer cell imaging. *Phys. Chem. Chem. Phys.* **2013**, *15*, 2961–2966. [CrossRef]
162. Klein, K.; Gigler, A.M.; Aschenbrenner, T.; Monetti, R.; Bunk, W.; Jamitzky, F.; Morfill, G.; Stark, R.W.; Schlegel, J. Label-free live-cell imaging with confocal Raman microscopy. *Biophys. J.* **2012**, *102*, 360–368. [CrossRef]
163. Geng, J.; Zhang, W.; Chen, C.; Zhang, H.; Zhou, A.; Huang, Y. Tracking the differentiation status of human neural stem cells through label-free Raman spectroscopy and machine learning-based analysis. *Anal. Chem.* **2021**, *93*, 10453–10461. [CrossRef]
164. Kallepitis, C.; Bergholt, M.S.; Mazo, M.M.; Leonardo, V.; Skaalure, S.C.; Maynard, S.A.; Stevens, M.M. Quantitative volumetric Raman imaging of three dimensional cell cultures. *Nat. Commun.* **2017**, *8*, 14843. [CrossRef]
165. Parrotta, E.; De Angelis, M.T.; Scalise, S.; Candeloro, P.; Santamaria, G.; Paonessa, M.; Coluccio, M.L.; Perozziello, G.; De Vitis, S.; Sgura, A. Two sides of the same coin? Unraveling subtle differences between human embryonic and induced pluripotent stem cells by Raman spectroscopy. *Stem Cell Res. Ther.* **2017**, *8*, 271. [CrossRef]
166. Lazarević, J.J.; Kukolj, T.; Bugarski, D.; Lazarević, N.; Bugarski, B.; Popović, Z.V. Probing primary mesenchymal stem cells differentiation status by micro-Raman spectroscopy. *Spectroc. Acta Pt. A-Molec. Biomolec. Spectr.* **2019**, *213*, 384–390. [CrossRef]
167. Hsu, C.-C.; Xu, J.; Brinkhof, B.; Wang, H.; Cui, Z.; Huang, W.E.; Ye, H. A single-cell Raman-based platform to identify developmental stages of human pluripotent stem cell-derived neurons. *Proc. Natl. Acad. Sci. USA.* **2020**, *117*, 18412–18423. [CrossRef]
168. Ralbovsky, N.M.; Dey, P.; Dey, B.K.; Lednev, I.K. Determining the stages of cellular differentiation using deep ultraviolet resonance Raman spectroscopy. *Talanta* **2021**, *227*, 122164. [CrossRef]
169. Mandair, G.S.; Steenhuis, P.; Ignelzi, M.A., Jr.; Morris, M.D. Bone quality assessment of osteogenic cell cultures by Raman microscopy. *J. Raman Spectrosc.* **2019**, *50*, 360–370. [CrossRef]
170. Alraies, A.; Canetta, E.; Waddington, R.J.; Moseley, R.; Sloan, A.J. Discrimination of dental pulp stem cell regenerative heterogeneity by single-cell Raman spectroscopy. *Tissue Eng. Part C-Methods* **2019**, *25*, 489–499. [CrossRef]
171. Simonović, J.; Toljić, B.; Rašković, B.; Jovanović, V.; Lazarević, M.; Milošević, M.; Nikolić, N.; Panajotović, R.; Milašin, J. Raman microspectroscopy: Toward a better distinction and profiling of different populations of dental stem cells. *Croat. Med. J.* **2019**, *60*, 78–86. [CrossRef]
172. Esmonde-White, F.W.L.; Morris, M.D. Raman imaging and Raman mapping. In *Emerging Raman Applications and Techniques in Biomedical and Pharmaceutical Fields*; Matousek, P., Morris, M.D., Eds.; Springer: Berlin/Heidelberg, Germany, 2010; pp. 97–110.
173. Ravera, F.; Efeoglu, E.; Byrne, H.J. Monitoring stem cell differentiation using Raman microspectroscopy: Chondrogenic differentiation, towards cartilage formation. *Analyst* **2021**, *146*, 322–337. [CrossRef]
174. De Bleye, C.; Fontaine, M.; Dumont, E.; Sacré, P.Y.; Hubert, P.; Theys, N.; Ziemons, E. Raman imaging as a new analytical tool for the quality control of the monitoring of osteogenic differentiation in forming 3D bone tissue. *J. Pharm. Biomed. Anal.* **2020**, *186*, 113319. [CrossRef]
175. Suhito, I.R.; Han, Y.; Ryu, Y.-S.; Son, H.; Kim, T.-H. Autofluorescence-Raman mapping integration analysis for ultra-fast label-free monitoring of adipogenic differentiation of stem cells. *Biosens. Bioelectron.* **2021**, *178*, 113018. [CrossRef]
176. Kim, H.; Han, Y.; Suhito, I.R.; Choi, Y.; Kwon, M.; Son, H.; Kim, H.-R.; Kim, T.-H. Raman spectroscopy-based 3D analysis of odontogenic differentiation of human dental pulp stem cell spheroids. *Anal. Chem.* **2021**, *93*, 9995–10004. [CrossRef]
177. Dou, X.; Zhao, Y.; Li, M.; Chen, Q.; Yamaguchi, Y. Raman imaging diagnosis of the early stage differentiation of mouse embryonic stem cell (mESC). *Spectrochim. Acta A Mol. Biomol. Spectrosc.* **2020**, *224*, 117438. [CrossRef]
178. Kukolj, T.; Lazarević, J.; Borojević, A.; Ralević, U.; Vujić, D.; Jauković, A.; Lazarević, N.; Bugarski, D. A single-cell Raman spectroscopy analysis of bone marrow mesenchymal stem/stromal cells to identify inter-individual diversity. *Int. J. Mol. Sci.* **2022**, *23*, 4915. [CrossRef]

179. Zong, C.; Xu, M.; Xu, L.-J.; Wei, T.; Ma, X.; Zheng, X.-S.; Hu, R.; Ren, B. Surface-enhanced Raman spectroscopy for bioanalysis: Reliability and challenges. *Chem. Rev.* **2018**, *118*, 4946–4980. [CrossRef] [PubMed]
180. Martines-Arano, H.; Palacios-Barreto, S.; Castillo-Cruz, J.; Meda-Campaña, J.A.; García-Pérez, B.E.; Torres-Torres, C. Fractional photodamage triggered by chaotic attractors in human lung epithelial cancer cells. *Int. J. Therm. Sci.* **2022**, *181*, 107734. [CrossRef]
181. Langer, J.; Jimenez de Aberasturi, D.; Aizpurua, J.; Alvarez-Puebla, R.A.; Auguié, B.; Baumberg, J.J.; Bazan, G.C.; Bell, S.E.J.; Boisen, A.; Brolo, A.G.; et al. Present and future of surface-enhanced Raman scattering. *ACS Nano* **2020**, *14*, 28–117. [CrossRef] [PubMed]
182. Liu, H.; Gao, X.; Xu, C.; Liu, D. SERS tags for biomedical detection and bioimaging. *Theranostics* **2022**, *12*, 1870. [CrossRef] [PubMed]
183. Mosier-Boss, P.A. Review of SERS substrates for chemical sensing. *Nanomaterials* **2017**, *7*, 142. [CrossRef] [PubMed]
184. Yang, B.; Jin, S.; Guo, S.; Park, Y.; Chen, L.; Zhao, B.; Jung, Y.M. Recent development of SERS technology: Semiconductor-based study. *ACS Omega* **2019**, *4*, 20101–20108. [CrossRef]
185. Song, C.; Guo, S.; Jin, S.; Chen, L.; Jung, Y.M. Biomarkers determination based on surface-enhanced Raman scattering. *Chemosensors* **2020**, *8*, 118. [CrossRef]
186. El-Said, W.A.; Kim, S.U.; Choi, J.-W. Monitoring in vitro neural stem cell differentiation based on surface-enhanced Raman spectroscopy using a gold nanostar array. *J. Mater. Chem. C* **2015**, *3*, 3848–3859. [CrossRef]
187. Shi, C.; Cao, X.; Chen, X.; Sun, Z.; Xiang, Z.; Zhao, H.; Qian, W.; Han, X. Intracellular surface-enhanced Raman scattering probes based on TAT peptide-conjugated Au nanostars for distinguishing the differentiation of lung resident mesenchymal stem cells. *Biomaterials* **2015**, *58*, 10–25. [CrossRef]
188. Alattar, N.; Daud, H.; Al-Majmaie, R.; Zeulla, D.; Al-Rubeai, M.; Rice, J.H. Surface-enhanced Raman scattering for rapid hematopoietic stem cell differentiation analysis. *Appl. Opt.* **2018**, *57*, E184–E189. [CrossRef]
189. Milewska, A.; Zivanovic, V.; Merk, V.; Arnalds, U.B.; Sigurjónsson, Ó.E.; Kneipp, J.; Leosson, K. Gold nanoisland substrates for SERS characterization of cultured cells. *Biomed. Opt. Express* **2019**, *10*, 6172–6188. [CrossRef]
190. D'Acunto, M. In situ surface-enhanced Raman spectroscopy of cellular components: Theory and experimental results. *Materials* **2019**, *12*, 1564. [CrossRef]
191. Wang, J.; Qi, G.; Qu, X.; Ling, X.; Zhang, Z.; Jin, Y. Molecular profiling of dental pulp stem cells during cell differentiation by surface enhanced Raman spectroscopy. *Anal. Chem.* **2020**, *92*, 3735–3741. [CrossRef]
192. Milewska, A.; Sigurjonsson, O.E.; Leosson, K. SERS imaging of mesenchymal stromal cell differentiation. *ACS Appl. Bio Mater.* **2021**, *4*, 4999–5007. [CrossRef]
193. Chen, X.; Li, X.; Yang, H.; Xie, J.; Liu, A. Diagnosis and staging of diffuse large B-cell lymphoma using label-free surface-enhanced Raman spectroscopy. *Spectrochim. Acta A Mol. Biomol. Spectrosc.* **2022**, *267*, 120571. [CrossRef]
194. Choi, J.-H.; Kim, T.-H.; El-said, W.A.; Lee, J.-H.; Yang, L.; Conley, B.; Choi, J.-W.; Lee, K.-B. In situ detection of neurotransmitters from stem cell-derived neural interface at the single-cell level via graphene-hybrid SERS nanobiosensing. *Nano Lett.* **2020**, *20*, 7670–7679. [CrossRef]
195. Omrani, M.; Mohammadi, H.; Fallah, H. Ultrahigh sensitive refractive index nanosensors based on nanoshells, nanocages and nanoframes: Effects of plasmon hybridization and restoring force. *Sci. Rep.* **2021**, *11*, 2065. [CrossRef] [PubMed]
196. Cao, X.; Wang, Z.; Bi, L.; Bi, C.; Du, Q. Gold nanocage-based surface-enhanced Raman scattering probes for long-term monitoring of intracellular microRNA during bone marrow stem cell differentiation. *Nanoscale* **2020**, *12*, 1513–1527. [CrossRef]
197. Hua, S.; Zhong, S.; Arami, H.; He, J.; Zhong, D.; Zhang, D.; Chen, X.; Qian, J.; Hu, X.; Zhou, M. Simultaneous deep tracking of stem cells by surface enhanced Raman imaging combined with single-cell tracking by NIR-II imaging in myocardial infarction. *Adv. Funct. Mater.* **2021**, *31*, 2100468. [CrossRef]
198. Riley, R.S.; Day, E.S. Gold nanoparticle-mediated photothermal therapy: Applications and opportunities for multimodal cancer treatment. *Wiley Interdiscip. Rev. Nanomed. Nanobiotechnol.* **2017**, *9*, e1449. [CrossRef]
199. Krafft, C.; Salzer, R.; Seitz, S.; Ern, C.; Schieker, M. Differentiation of individual human mesenchymalstem cells probed by FTIR microscopic imaging. *Analyst* **2007**, *132*, 647–653. [CrossRef]
200. Downes, A.; Mouras, R.; Elfick, A. Optical spectroscopy for noninvasive monitoring of stem cell differentiation. *J. Microbiol. Biotechnol.* **2010**, *2010*, 101864. [CrossRef]
201. Wang, Y.; Dai, W.; Liu, Z.; Liu, J.; Cheng, J.; Li, Y.; Li, X.; Hu, J.; Lü, J. Single-cell infrared microspectroscopy quantifies dynamic heterogeneity of mesenchymal stem cells during adipogenic differentiation. *Anal. Chem.* **2021**, *93*, 671–676. [CrossRef]
202. Gieroba, B.; Przekora, A.; Kalisz, G.; Kazimierczak, P.; Song, C.L.; Wojcik, M.; Ginalska, G.; Kazarian, S.G.; Sroka-Bartnicka, A. Collagen maturity and mineralization in mesenchymal stem cells cultured on the hydroxyapatite-based bone scaffold analyzed by ATR-FTIR spectroscopic imaging. *Mater. Sci. Eng. C* **2021**, *119*, 111634. [CrossRef]
203. Kato, N. Optical second harmonic generation microscopy: Application to the sensitive detection of cell membrane damage. *Biophys. Rev.* **2019**, *11*, 399–408. [CrossRef]
204. Qi, X.; Liu, H.; Guo, W.; Lin, W.; Lin, B.; Jin, Y.; Deng, X. New opportunities: Second harmonic generation of boron-doped graphene quantum dots for stem cells imaging and ultraprecise tracking in wound healing. *Adv. Funct. Mater.* **2019**, *29*, 1902235. [CrossRef]

205. Ibrahim, A.; Rodriguez-Florez, N.; Gardner, O.F.W.; Zucchelli, E.; New, S.E.P.; Borghi, A.; Dunaway, D.; Bulstrode, N.W.; Ferretti, P. Three-dimensional environment and vascularization induce osteogenic maturation of human adipose-derived stem cells comparable to that of bone-derived progenitors. *Stem Cell Res. Ther.* **2020**, *9*, 1651–1666. [CrossRef] [PubMed]
206. Kourgiantaki, A.; Tzeranis, D.S.; Karali, K.; Georgelou, K.; Bampoula, E.; Psilodimitrakopoulos, S.; Yannas, I.V.; Stratakis, E.; Sidiropoulou, K.; Charalampopoulos, I.; et al. Neural stem cell delivery via porous collagen scaffolds promotes neuronal differentiation and locomotion recovery in spinal cord injury. *Regen. Med.* **2020**, *5*, 12. [CrossRef] [PubMed]
207. Bertani, F.R.; Ferrari, L.; Mussi, V.; Botti, E.; Costanzo, A.; Selci, S. Living matter observations with a novel hyperspectral supercontinuum confocal microscope for VIS to near-IR reflectance spectroscopy. *Sensors* **2013**, *13*, 14523–14542. [CrossRef] [PubMed]
208. Ogi, H.; Moriwaki, S.; Kokubo, M.; Hikida, Y.; Itoh, K. Label-free classification of neurons and glia in neural stem cell cultures using a hyperspectral imaging microscopy combined with machine learning. *Sci. Rep.* **2019**, *9*, 633. [CrossRef]
209. Mehta, N.; Shaik, S.; Prasad, A.; Chaichi, A.; Sahu, S.P.; Liu, Q.; Hasan, S.M.A.; Sheikh, E.; Donnarumma, F.; Murray, K.K.; et al. Multimodal label-free monitoring of adipogenic stem cell differentiation using endogenous optical biomarkers. *Adv. Funct. Mater.* **2021**, *31*, 2103955. [CrossRef]